M. AHMED

ATILIM UNIVERSITY 2023

UNDERSTANDING THE DIVERSITY AMONG HUMAN URINES USING AN ARTIFICIAL URINE SYSTEM AND FTIR SPECTROSCOPY

THE GRADUATE SCHOOL OF NATURAL AND APPLIED SCIENCES
OF
ATILIM UNIVERSITY

MARIAM HANY FAROUK MOHAMED AHMED

A MASTER OF SCIENCE THESIS
IN
THE DEPARTMENT OF PHYSICS

JANUARY 2023

UNDERSTANDING THE DIVERSITY AMONG HUMAN URINES USING AN ARTIFICIAL URINE SYSTEM AND FTIR SPECTROSCOPY

A THESIS SUBMITTED TO
THE GRADUATE SCHOOL OF NATURAL AND APPLIED SCIENCES
OF
ATILIM UNIVERSITY

BY

MARIAM HANY FAROUK MOHAMED AHMED

IN PARTIAL FULFILLMENT OF THE REQUIREMENTS
FOR
THE DEGREE OF MASTER OF SCIENCE
IN
THE DEPARTMENT OF PHYSICS

JANUARY 2023

Approval of the Graduate School of Natural and Applied Sciences, Atılım University.

_____

Prof. Dr. Ender KESKİNKILIÇ
Director

I certify that this thesis satisfies all the requirements as a thesis for the degree of **Master of Science in Applied Physics, Atılım University**.

_____

Prof. Dr. Mehmet Işık
Head of Department

This is to certify that I have read the thesis UNDERSTANDING THE DIVERSITY AMONG HUMAN URINES USING AN ARTIFICIAL URINE SYSTEM AND FTIR SPECTROSCOPY submitted by MARIAM HANY FAROUK MOHAMED AHMED and that in my opinion it is fully adequate, in scope and quality, as a thesis for the degree of Master of Science.

_____

Prof. Dr. Filiz Korkmaz Özkan
Supervisor

Examining Committee Members:

Prof. Dr. Mehmet Işık
Department of Physics, Atılım University _____

Prof. Dr. Filiz Korkmaz Özkan
Department of Physics, Atılım University _____

Dr. Neslihan Sarıgül
Institute of Nuclear Sciences, Hacettepe University _____

Date: *13.01.2023*

I hereby declare that all information in this document has been obtained and presented in accordance with academic rules and ethical conduct. I also declare that, as required by these rules and conduct, I have fully cited and referenced all material and results that are not original to this work.

Mariam Hany Farouk Mohamed, Ahmed:

Signature:

ABSTRACT

UNDERSTANDING THE DIVERSITY AMONG HUMAN URINES USING AN ARTIFICIAL URINE SYSTEM AND FTIR SPECTROSCOPY

Ahmed, Mariam Hany Farouk Mohamed

M.S., Department of Applied Physics

Supervisor: Prof. Dr. Filiz Korkmaz Özkan

January 2023, 44 pages

Urine tests are a common and convenient way to identify and diagnose a variety of disorders. In this study, we employ a novel artificial urine protocol (MP-AU) to determine the spectra of the normal minimum and maximum values of 9 urine components within the normal physiological range. Fourier Transform Infrared (FTIR) spectroscopy is employed to generate these spectra, which will aid in the early detection of disorders, if any exists.

The spectrum obtained from the patient's urine sample would be compared to the spectra obtained from artificial urine solutions for the minimum and maximum normal values. The outcome of this comparison will be related to the patient's health. If the patient's spectrum lies between these two normal spectra, the patient can be considered healthy. Correspondingly, if the patient's spectrum falls outside of the normal range, more tests can be ordered to detect the anomaly.

The findings of this study reveal that the quantity of components within the artificial urine system is correlated with the amplitudes of the peaks in the FTIR spectra. Furthermore, characteristic peak positions of the tested urine components are identified, which can be used as a reference in further studies.

This study was financially supported by Atilim University Research Support program, Grant number ATU-ADP-2122-01.

Keywords: FTIR spectroscopy, normal range, artificial urine, Urinalysis, urine components.

ÖZ

İNSAN İDRARLARI ARASINDA GÖZLENEN ÇEŞİTLİLİĞİN YAPAY İDRAR SİSTEMİ VE FTIR SPEKTROSKOPİSİ KULLANILARAK ANLAŞILMASI

Ahmed, Mariam Hany Farouk Mohamed
Yüksek Lisans, Uygulamalı Fizik Bölümü
Tez Yöneticisi : Prof. Dr. Filiz Korkmaz Özkan

Ocak 2023, 44 sayfa

İdrar testleri, çeşitli tıbbi bozuklukları tanımlamanın ve teşhis etmenin yaygın ve uygun bir yoludur. Bu çalışmada, 9 yapay idrar bileşeninin normal minimum ve maksimum değerlerinin spektrumunu belirlemek için yeni bir yapay idrar protokolünü (MP-AU) kullanıyoruz. Fourier Transform Infrared (FTIR) spektroskopisi, varsa bozuklukların erken saptanmasına yardımcı olacak bu spektrumları oluşturmak için kullanılmıştır.

Hastanın idrar numunesinden elde edilen spektrum, minimum ve maksimum normal değerler için yapay idrar çözeltilerinden elde edilen spektrumlarla karşılaştırılabilir. Bu karşılaştırmanın sonucu hastanın sağlığı ile ilgili olacaktır. Hastanın spektrumu bu iki normal spektrum arasında yer alıyorsa, hastanın sağlık olduğu düşünülebilir. Buna bağlı olarak, hastanın spektrumu normal aralığın dışına çıkarsa, anomaliyi saptamak için daha fazla test istenebilir.

Bu çalışmanın bulguları, yapay idrar sistemi içindeki bileşenlerin miktarının, FTIR spektrumundaki tepe noktalarının genlikleri ile ilişkili olduğunu ortaya koymaktadır. Ayrıca, daha sonraki çalışmalarda referans olarak kullanılmak üzere, test edilen idrar bileşenlerinin karakteristik bant pozisyonları da belirlenmiştir.

Bu çalışma Atılım Üniversitesi Araştırma Destek programı çerçevesinde ATÜ-ADP-2122-01 numaralı proje ile finansal olarak desteklenmiştir.

Anahtar Kelimeler: FTIR spektroskopisi, normal aralık, yapay idrar, idrar tahlili, idrar bileşenleri.

DEDICATION

To my beautiful family…

ACKNOWLEDGMENTS

I would like to express my gratitude to my supervisor Prof. Dr. Filiz Korkmaz Özkan for providing me with great input into this work. She gave me the greatest opportunity to do research on such an important topic, as well as encouragement, dedication, and continuous support throughout the course of the Master program. I also want to thank Dr. Neslihan Sarıgül for helping and teaching me the laboratory skills for conducting my experiments.

I shall also thank my family for their understanding and sharing so many hours, which were rightfully theirs. Without their encouragement and love, this work could not have been completed.

I sincerely thank the head of Applied Physics Department Prof. Dr. Mehmet Işık.

I am also thankful to all the instructors and all the faculty members in the Applied Physics Department for providing good academic lectures; especially Applied Physics group who have directly or indirectly helped me during the project work.

TABLE OF CONTENTS

LIST OF TABLES

LIST OF FIGURES

LIST OF SYMBOLS/ABBREVIATIONS

ATR	Attenuated Total Reflectance
DTGS	Deuterated Tri Glycine Sulphate
FTIR	Fourier Transform Infrared
GFR	Glomerulus Filtration Rate
HPF	High Powered Field
IR	Infrared
MCT	Mercury Cadmium Telluride
MP-AU	Multipurpose Artificial Urine
NFP	Net Filtration Pressure
RBCs	Red Blood Cells
UA	Urinalysis
WBCs	White Blood Cells

CHAPTER 1

INTRODUCTION

1.1 Urine Formation

Urine is a waste fluid produced by the human body through the kidneys [1]. This fluid consists mainly of water (95%), urea (2%) and other components such as creatinine, uric acids, and ions that add up to 3% in total [2]. The system that is responsible for eliminating urea from the body, maintaining acid-base balance, sustaining hemodynamics, and getting rid of other unnecessary substances is called the urinary system. The main organs in this system are the two kidneys, the two ureters, the urinary bladder, and the urethra (Figure 1.1). Eliminating unnecessary and toxic substances from the body occurs in three main processes; glomerular filtration, reabsorption, and secretion. The first process, i.e. glomerular filtration, depends on nephrons, the kidneys' functional units (Figure 1.2) [3].

The renal corpuscle is the structure essential for the filtration of blood in the kidney's nephron. The glomerulus is the first part of the renal corpuscle, which is the network of specialized capillaries. The second part of the renal corpuscle is the Bowman's capsule which collects the filtrates and transports them to the proximal convoluted tubule. The blood enters the glomerulus from the afferent arteriole and exits via the efferent arteriole. The fluid that enters the glomerulus is called glomerulus filtrate. The filtration here occurs across an ultrafiltration barrier. Due to this barrier, molecules with a diameter of less than 1.8 nanometer are filtered out, but those molecules larger than 3.6 nanometers cannot be filtered.

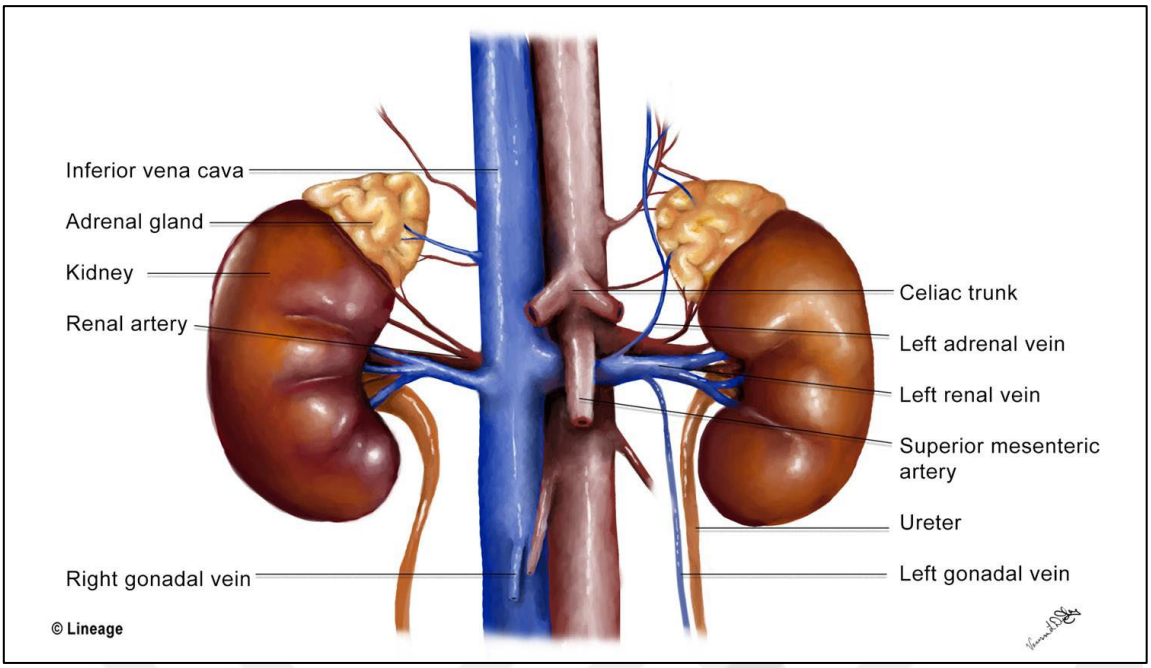

Figure 1.1 Anatomy of the excretory system [4]

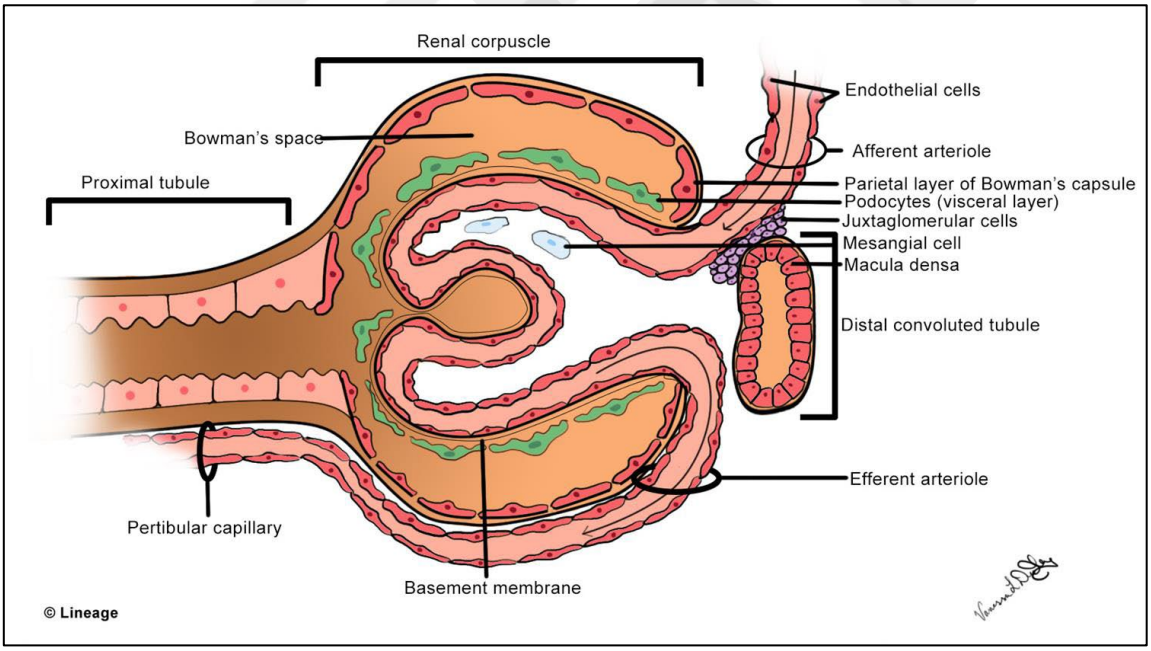

Figure 1.2 Anatomy of nephron [4]

The ultrafiltration barriers consist of three layers. These three layers are all negatively charged with glycoproteins. Due to the negatively charged glycoproteins, negative molecules cannot pass through this barrier. For example, serum albumin cannot be filtered even if it fits in size range. The bottom layer is the endothelium of the capillary, which contains pores called fenestrations. All molecules can pass through this layer, such as salts, water, and sugar, due to their small size, unlike blood cells, which cannot pass through due to their larger size. These large molecules stay in the capillary and generate osmotic pressure within the capillary. The middle layer is the basement membrane which prevents the filtration of large proteins. The last layer is the outer layer consisting of podocytes. These podocytes have many finger-like projections which are so close to each other called pedicels. This part has narrow filtration slits, which allow only the small molecules to pass through [3]. Ultrafiltration of blood depends on the balance between two forces: hydrostatic pressure and oncotic pressure.

Hydrostatic pressure is a force that the fluid does on the walls of its compartment, which in this case is the Bowman's capsule. On the other hand, oncotic pressure is pressure due to the force of plasma proteins on the walls of its capillaries. So, the net filtration pressure (NFP) is equal to the hydrostatic pressure of the glomerulus capillary (55 mmHg) minus the hydrostatic pressure of Bowman's capsule (15 mmHg) minus oncotic pressure of glomerulus capillary protein (30 mmHg) which is equal (10 mmHg) [5]. As there are many nephrons and renal corpuscles in the two kidneys, this rate is called the glomerulus filtration rate (GFR). It indicates how much filtrate is formed by all the renal corpuscles in the two kidneys per minute. GFR is used to know how well the two kidneys are working. The normal GFR is 90 ml/min/1.73 m^2 [6].

Blood coming from the renal artery enters the glomerulus from the afferent arteriole. After being filtrated in the glomerulus, this blood has two ways to exit: either it flows out as blood through the efferent arteriole or exits as filtrate from the glomerulus. This filtrate is not blood because it should not contain red blood cells or large proteins such as albumin, so it is mainly water with small solutes. When the afferent arteriole is vasoconstricted, less blood can enter the glomerulus. Due to this fact, less filtrate will be produced. Due to vasoconstriction, the vascular resistance will

increase, and there will be lesser renal blood volume. Because of this, there will be less pressure in the glomerulus, and the GFR will be decreased.

On the other hand, when the efferent arteriole is vasoconstricted, the blood can easily enter the glomerulus through the afferent arteriole as it is now not vasoconstricted but exits hardly from the efferent arteriole. Due to this, increased pressure in the glomerulus will lead to a higher amount of filtrate than normal. So, the GFR will be increased even if there is still vascular resistance [7].

The filtrate that enters the nephron consists of water and various solutes. The main reason for urine formation is to remove waste elements such as creatinine and urea from the circulation before they become toxic. If the two kidneys work well, the body produces a filtrate of about 90 ml/min / 1.73 m^3. First, in the proximal convoluted tubule, potassium, sodium chloride, water, amino acids, glucose and bicarbonate reabsorption occurs. Potassium, sodium chloride, and water are reabsorbed by 65%, whereas amino acids and glucose are reabsorbed by 100%. These components are helpful and essential for the human body, so it would be wasteful to get rid of them out of the body.

On the other hand, bicarbonate is reabsorbed by 90% because if it is excreted from the body in massive amounts, this causes the body to be more acidic than normal. Uric acid, a nitrogenous waste, and organic acids, which contain many antibiotics, are secreted into the proximal convoluted tubule. The next part is the loop of Henle, which is responsible for urine concentration. In the descending limb of the loop, water is reabsorbed due to the water permeability of this part. On the other hand, in the ascending limb, 25% of filtered sodium chloride is reabsorbed. However, there are high concentrations of other waste components, such as urea. In the distal convoluted tubule, 5% of filtered sodium chloride is absorbed. From the previous information, the reabsorption of the water in the nephron depends on the sodium chloride's movement, which happens due to osmotic pressure. Also, potassium and hydrogen ions are secreted in the distal tubule, which means they are moved back into the nephron.

In conclusion, the proximal convoluted tubule is responsible for most of the reabsorption and secretion processes, whereas the loop of Henle is responsible for urine concentration. On the other hand, the distal tubule does fine-tuning. Therefore,

urea and some of the filtered sodium chloride are reabsorbed in the last part, the collecting duct (Figure 1.3) [8]. Creatinine is a sign of glomerular filtration rate as it is not reabsorbed from the secretion through the nephron. So, if creatinine increases in the blood, there may be a problem in the glomerulus. The last step is excretion, where the components of the urine go out from the nephron to the urethra and then to the urinary bladder. The significant components of urine are water, sodium chloride, potassium, bicarbonate, creatinine and urea [8].

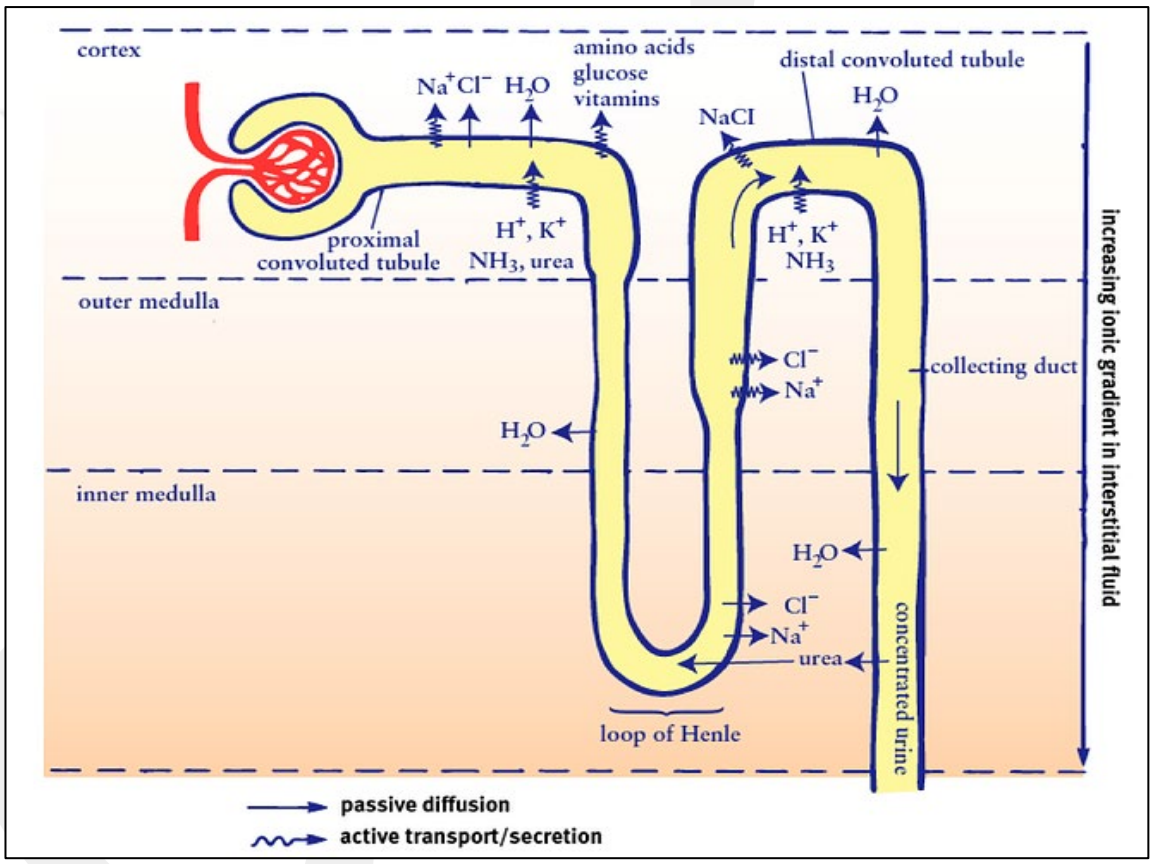

Figure 1.3 Labeled diagram of a nephron [9]

In previous studies using mass spectroscopy, approximately 250 different solutes are routinely excreted from the human body with urine. On the other hand, depending on the person's diet and the time in which the sample of urine is taken, there can be approximately 3000 solutes in the urine (Figure 1.4) [1], [2].

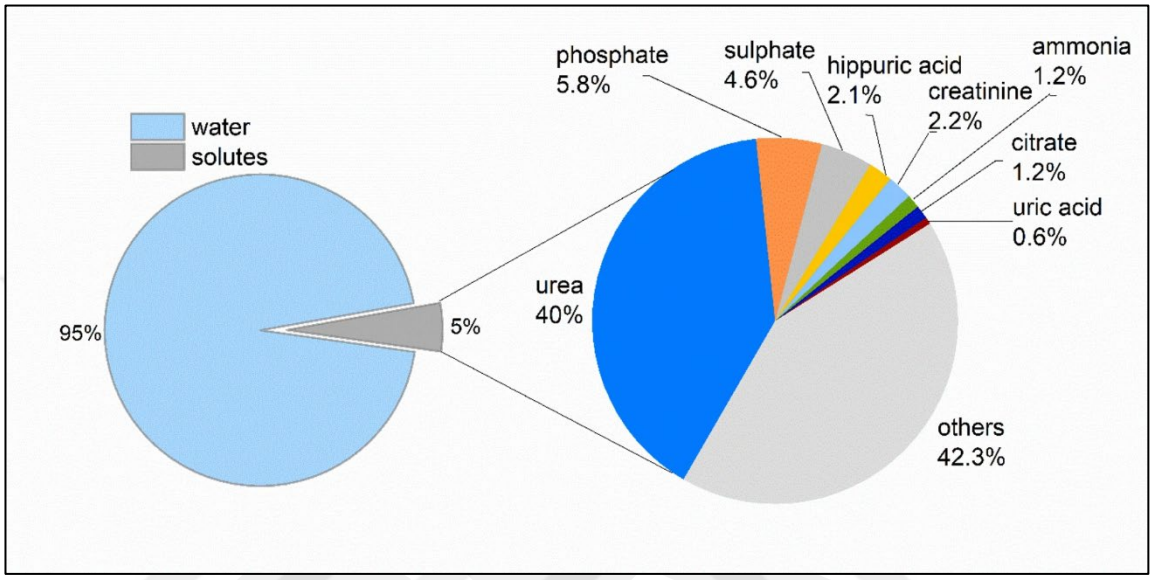

Figure 1.4 The composition of human urine. The percentages reflect the mass ratio of each urine component with respect to the total mass of 1.5 L-urine. The others (42.3%) represent hundreds of different molecules, each contributing less than 0.5% to the total urine composition in the same chart. The picture is taken from Kurultak et al., 2022 [2], with authors' permission

1.2 Current Clinical Methods of Testing Urine

Urinalysis (UA) tests on a urine sample indicate several health problems, such as kidney failure, urinary tract infections, kidney stones and acid-base disorders [10]. Urinalysis can be divided into three sections: visual examination; dipstick, and urine microscopy.

Firstly, urine color indicates the degree of hydration. For example, if the color of the urine sample is amber-yellow, that may indicate dehydration. On the other hand, the color of the urine is also affected by health conditions, the kind of medicine the patient takes, or the diet the patient follows. For example, red color may refer to bleeding from the kidneys or the urethra or even the ureters. Also, the red color may

refer to the diet of the patient who had beets or other same fruits and vegetables. The orange color of the urine may refer to a high level of bilirubin in the body which may be caused by liver disease; it can also refer to the type of antibiotic called rifampin. The last example is the green color, which is not common, may refer to urinary tract infection due to Pseudomonas or excess digestion of food with blue dye like asparagus [11]. Secondly, the turbidity of urine means how clear it is. Normal urine must be clear, so if it is turbid, it may refer to urinary tract infections or the presence of crystals [12].

The second section is the urine dipstick, a reagent strip with pads on it. These pads are sensitive to different components in the urine. The dipstick test is easy to use. Firstly, the strip is dipped in the urine or soaked with the urine using a pipette. Then the excess urine is wiped off, and the strip is left for 1-2 minutes. Incubation time depends on the instructions from the manufacturing company. At this point, pads on the strip are compared with the list of the color of different components of the urine that comes with the strips. Each color indicates the amount of components in the urine semi-quantitatively. The first of these components is specific gravity. The specific gravity is the ratio of the urine's density to that of the water. Although water is the main component in urine, urine is always denser. This density comes from the urea, electrolytes and other components found in the urine. The normal range of specific gravity is from 1.005 to 1.030. For example, if the specific gravity is approximately 1.001, that refers to excessive hydration or maybe diabetes insipidus. On the other hand, if it is close to 1.035 it may refer to dehydration, glycosuria or proteinuria. The second component that the dipstick test reveals is the urinary pH. The pH ranges from 4.5 to 8, depending on the patient's health conditions. If pH is lower than or equal to 5, it may indicate excessive lactate or ketones. If pH is between 7 and 8, it may refer to alkalemia or urinary tract infections. Although this test is important, it cannot be used without knowing the diet the patient follows because pH is highly affected by the patient's diet.

The next component is glucose, and any glucose in this test refers to glycosuria as glucose, which the proximal convoluted tubule must completely reabsorb. The dipstick test is susceptible to hemoglobin. If there is urinary blood, it may be an indication of renal stones or urinary tract infections. Also, dipstick for protein is

sensitive to albumin. This sensitivity depends on its concentration in urine. If albumin is detected in this test, it refers to a glomerular disease. Another component is the leukocytes which refer to the white blood cells in the urinary tract. The presence of nitrites in this test refers to Enterobacteriaceae. On the other hand, the presence of ketones may refer to diabetics or prolonged hunger. The last test that the dipstick can do is bilirubin and urobilinogen. For example, in the case of hemolysis, the level of urobilinogen increases in the urine. In another case of biliary obstruction, the level of bilirubin increases and the level of urobilinogen may decrease [13].

The third type of urine analysis is urine microscopy. In this section sample of urine must be prepared in a few steps. Firstly, at least 10 ml of urine is centrifuged for 5 minutes. After this time, a liquid layer will float on the top of the tube (supernatant) and the high molecular weight components of the urine will remain at the bottom of the tube (pellet). The supernatant is discarded and the pellet is homogenized by shaking the tube. Next, a sample is taken, applied on a microscope slide with a coverslip, and placed under a microscope [14]. the time and way of storing the urine sample are necessary to be recorded because they affect the interpretation of the results. For example, if the urine is left for a long time, the cells or crystals may start to breakdown and thus give misleading results. The first component seen under the microscope is the red blood cells (RBCs). RBCs are defined in the urine test by the number of cells per high-powered field, which in most cases equals 400x. To say that there are abnormal RBCs in the urine sample, it must be more than or equal to 3 per this high-powered field. In this case, the most vital suggestion is a glomerular disease, or it may also be a urinary tract infection [15]. The second component is the white blood cells which are similarly defined as the number of cells per high-powered field. The result is abnormal if it is more than 5, and there are many reasons for this abnormality, one of which is urinary tract infections [16]. The third component is the presence of bacteria. The presence of bacteria in the urine is evidence of urinary tract infections [17]. The fourth component is the crystals, microscopic solids composed of ions, molecules, or both. The formation of these crystals depends on the concentration of the ions and molecules in the urine and the pH of the urine. One of these crystals which may appear under the microscope is the uric acid crystals. They are formed due to the acidic urine and are related strongly to tumor lysis syndrome. Also, calcium phosphate crystals may appear

in this test, related to alkaline urine. Magnesium, ammonium, and phosphate crystals can be seen in alkaline urine when ammonium concentration is high. Calcium oxalate can be seen in two cases, and these crystals do not depend on the pH of the urine. The first case is the calcium oxalate dehydration crystals, and the second case is the calcium oxalate monohydrate crystals, and this type may refer to ethylene glycol ingestion (Table 1.1) [18], [19].

Table 1.1 Physical and biochemical properties of a healthy urine sample [20]

<table>
<tr><th colspan="2">Physical characteristics</th><th colspan="2">Chemical characteristics</th><th colspan="2">Microscopic characteristics</th></tr>
<tr><td>Color</td><td>Amber</td><td>Blood</td><td>Negative</td><td>RBCs</td><td>0 to 3 RBCs/HPF</td></tr>
<tr><td>Turbidity</td><td>Clear</td><td>Glucose</td><td>Negative</td><td>WBCs</td><td>0 to 4 WBCs/HPF</td></tr>
<tr><td>pH</td><td>4.5 to 8.0</td><td>Ketones</td><td>Negative</td><td>Epithelial cells</td><td>0 to 3/ HPF</td></tr>
<tr><td rowspan="5">Specific gravity</td><td rowspan="5">1.015 to 1.025</td><td>Protein</td><td>Negative</td><td>Casts</td><td>Negative</td></tr>
<tr><td>Bilirubin</td><td>Negative</td><td>Crystals</td><td>Negative</td></tr>
<tr><td>Urobilinogen</td><td>Negative</td><td rowspan="3">Bacteria</td><td rowspan="3">Negative</td></tr>
<tr><td>Leucocyte esterase</td><td>Negative</td></tr>
<tr><td>Nitrite for bacteria</td><td>Negative</td></tr>
</table>

1.3 Electromagnetic Spectrum

The electromagnetic spectrum is the range of frequencies light can have from radio waves to gamma rays (Figure 1.5). All of these waves travel with the speed of light, which can be calculated from the equation:

$$c = \lambda . \nu \quad , c = 3 \times 10^8 \, m/s \tag{1.1}$$

In the electromagnetic spectrum, the wavelength increases as going toward radio waves. On the other hand, as going towards the gamma rays, the frequency increases. The energy of photons in these waves is directly proportional to the frequency. The energy of photons can be determined as the following:

$$E = h . \nu \quad , h \; is \; Plank's \; constant = 6.626 \times 10^{-34} \; Joule . second \tag{1.2}$$

For example, gamma rays have the highest frequency and thus are the most energetic photons in the electromagnetic spectrum [21].

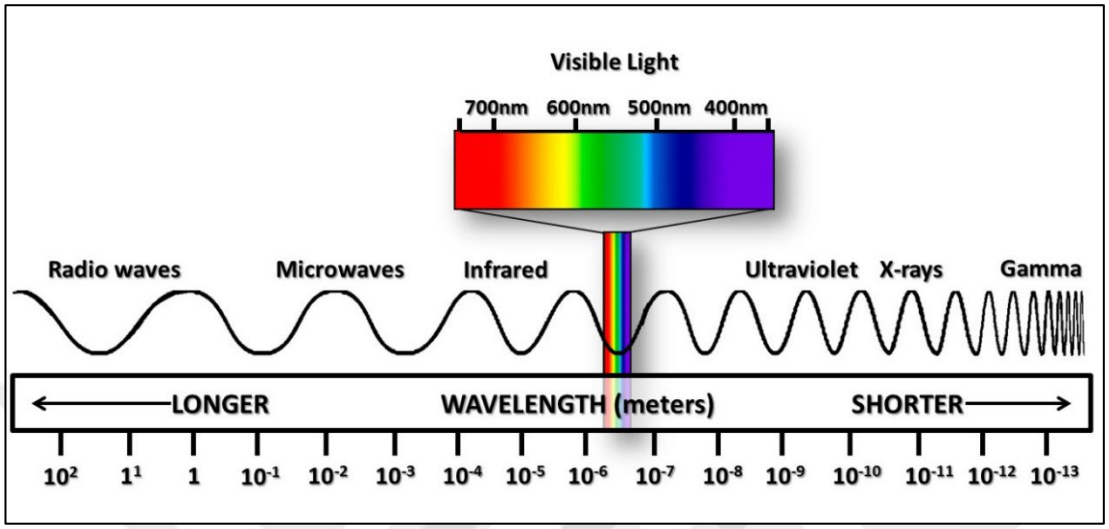

Figure 1.5 Electromagnetic spectrum [22]

Infrared is also part of electromagnetic radiation that has a longer wavelength than visible light, which extends from 700 nm to 1 mm. It is also called heat radiation because it has the property of heating objects when it falls on or is emitted from them [23]. This type of radiation is not energetic enough to excite electrons or to break down the chemical bonds between molecules, but it causes molecules to vibrate. So, this vibrational energy is eventually reemitted as heat. The infrared part of the electromagnetic spectrum is divided and analyzed in three different regions, classified according to their wavelength, ranging into near infrared, mid infrared, and far infrared. This window of the spectrum emitted from substances provides information about the vibrational states of the composing molecules. Every atom and molecular group have their characteristic vibrational frequencies; thus, measurement of emitted infrared radiation allows the identification of molecules making up the substances [24].

1.4 Interaction Between Light and Matter

According to Bohr's model of the atom, electrons can be only found at certain discrete energy levels. The difference between any two levels of these energy levels is ΔE. The electron can move from a lower to a higher energy level by absorbing energy from a photon equal to ΔE. When this electron returns to its original energy level, it emits this energy again as a photon (Figure 1.6) [25]. Combining the wavelength-frequency equation and that of the energy of a photon, the energy of a photon can be expressed as:

$$E = \frac{h.c}{\lambda} \tag{1.3}$$

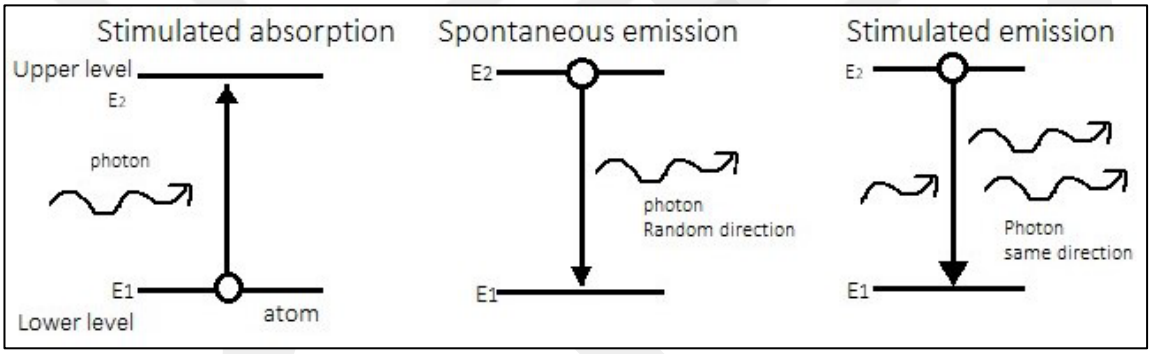

Figure 1.6 The interaction between an atom and a photon [26]

The middle infrared zone extends from 400 to 4000 cm^{-1}, and according to the equation of photon energy, it is proportional to the frequency and inversely proportional to the wavelength (Table 1.2).

Table 1.2 The photon energy of the middle infrared zone, its wavelength and frequency

Wavenumber (cm^{-1})	**Wavelength (nm)**	**Frequency (Hz)**	**Photon energy (eV)**
4000	2500	1.2×10^{14}	0.4963
400	25000	1.2×10^{13}	0.0496

1.5 States of Energy Within the Molecules

A molecule in the ground state has three types of energies. The first is due to the electrons inside the molecule, called electronic energy. The second is due to the vibrations within the molecule, called vibrational energy. The last is due to the molecule's rotation, called rotational energy. When this molecule is irradiated with a source of light, this source supplies the energy that is equal to that of the energy gap between two electronic states. Each spectroscopic technique can detect one type of these energy states. For example, the UV-spectroscopy detects the electronic transition, while infrared spectroscopy detects the vibrational transitions, and that is because infrared has less energetic radiation than that of ultraviolet. The molecules' bonds are flexible, so they can act like springs. If these bonds got enough energy, they could be stretched or compressed. On the other hand, this energy can also change the angle between bonds, which makes one of the atoms bend relative to another. A source of infrared radiation can supply this energy. If the length of the bond is changed, this is called a stretching vibration, while if the angle between bonds changed, this is called bending vibration. Stretching vibration can be divided into two types as symmetric and asymmetric. On the other hand, bending vibration can be divided into in-plane and out-of-plane bending (Figure 1.7) [27]. For a molecule to be active, it should change its net dipole moment; consequently, not all molecules are active.

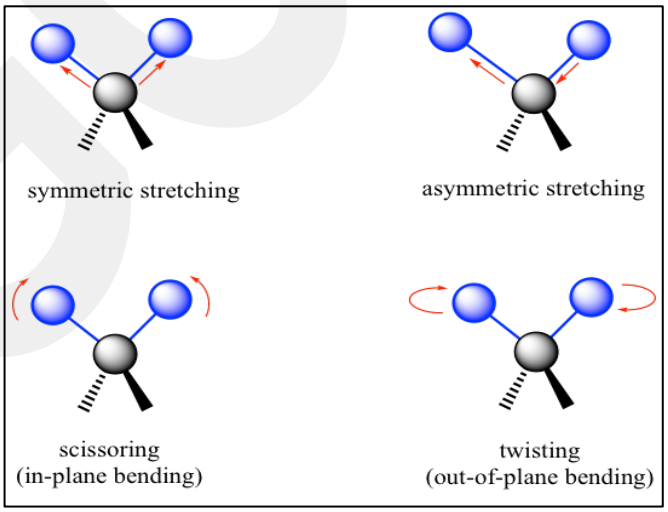

Figure 1.7 Vibration Modes of Bonds [28]

1.6 The Dipole Moment

The electric dipole moment is defined as two charges $(+q, -q)$ equal in magnitude and opposite in their sign with a distance between them called (d) (Figure 1.8). The separation distance is also called the dipole axis. The magnitude of the electric dipole moment can be calculated from the next equation:

$$\vec{P} = q.\vec{d} \tag{1.4}$$

If the dipole is placed inside an electric field and its axis is horizontal, the positive charge will be affected by force accelerating it along the electric field direction. On the other hand, the negative charge will also be affected by a force that accelerates it in the opposite direction of the electric field. As the two charges are equal in magnitude and opposite in their sign, the net force on the dipole is zero. In another case, if the dipole is placed in an electric field where its axis is perpendicular to the electric field, both charges will be affected by two forces opposite in direction. In this case, the axis of the dipole will rotate around its center under the effect of torque [29]. Torque, in this case, can be calculated using the following equation:

$$\tau = F.d \tag{1.5}$$

The force acting on the charge can be calculated as follows:

$$\vec{F} = q.\vec{E} \tag{1.6}$$

So the net torque can be calculated as:

$$\tau = q.E.d \tag{1.7}$$

After a time of rotating, the axis of the dipole will make an angle with the electric field. In this case, the net torque can be calculated as the following equation:

$$\tau = E.q.d.\sin\theta \tag{1.8}$$

Also, this equation can be rewritten as:

$$\tau = \vec{P} \times \vec{E} \tag{1.9}$$

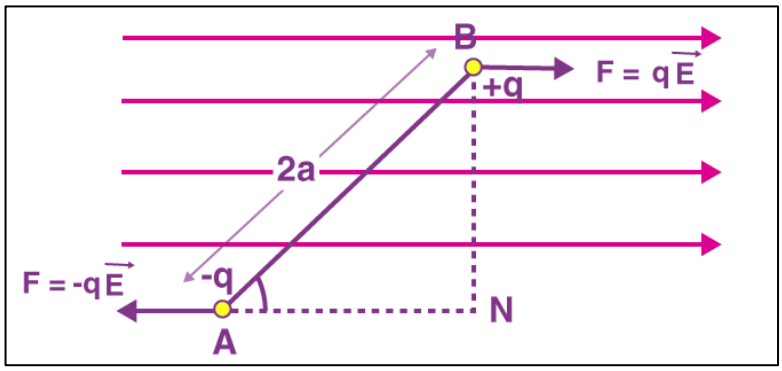

Figure 1.8 The electric dipole moment [30]

1.7 Infrared Active Molecules

The covalent bonds act as vibrating springs. If there is a change in the dipole moment of these bonds, like stretching or compression, then they are called infrared active. In this case, these bonds produce peaks in the spectrum when spectroscopy is used. Vibration energy depends on the strength of the bond (bond order) forming the molecule, and the two are directly proportional, i.e., as the bond strength increases, absorption frequency (wavenumber) increases as well (Table 1.3) [29]. On the other hand, if there is no change in the dipole moment, they are called infrared inactive.

Table 1.3 Examples of the relation between the absorption frequency and the strength of the bond

Bond	**Wavenumber (cm^{-1})**	**Bond**	**Wavenumber (cm^{-1})**	**Bond**	**Wavenumber (cm^{-1})**
$C-C$	~1200	$C-O$	~1110	$C-N$	~1135
$C=C$	~1660	$C=O$	~1750	$C=N$	~1665
$C\equiv C$	~2200	$C\equiv O$	~2100	$C\equiv N$	~2240

1.8 FTIR Spectroscopy

Fourier transform infrared (FTIR) spectroscopy is a technique used to identify and analyze the chemical composition of a sample by measuring the sample's infrared (IR) absorbance spectra. Based on the principle that different molecules absorb specific wavelengths of IR radiation differently, this variation can be used to identify and quantify the different chemical bonds and functional groups present in the sample. In an FTIR spectrometer, a sample is irradiated with a beam of IR radiation. Some of the radiation is absorbed by the sample, while the rest passes through and is detected by a detector. The absorbance spectrum of the sample is then obtained by plotting the sample's absorbance (or transmittance) at various wavelengths of IR radiation. FTIR spectroscopy is widely used in various fields, including materials science, pharmaceuticals, environmental science, and polymer chemistry, to name a few. It is a fast, non-destructive, and susceptible technique that can identify and quantify many molecules, including organic compounds, inorganic compounds, and polymers [31].

1.9 Beer-Lambert Law

The Beer-Lambert law, also known as the Beer-Lambert-Bouguer law or the Lambert-Beer law, is an empirical law that describes the relationship between the absorbance of a substance and the concentration of that substance in a solution. It states that the absorbance of a solution is directly proportional to the concentration of the absorbing species in the solution, and the path length of the light through the solution. Mathematically, the Beer-Lambert law is expressed as:

$$A = \varepsilon bc \tag{1.10}$$

Where: (A) Is the absorbance, (ε) is molar absorptivity (a measure of how well a compound absorbs a given wavelength of light), (b) is path length (a distance that light has to travel through a sample) and (c) is the concentration of the sample (the more concentration, the more absorbance that will occur). The Beer-Lambert law is widely used in analytical chemistry to determine the concentration of a species in a solution. It is often used in conjunction with spectroscopic techniques, such as UV-vis spectroscopy, to determine the concentration of a substance in a solution. It is a simple

yet powerful tool with many applications in various fields, including environmental science, pharmaceuticals, and food science [32].

1.10 FTIR Components

A Fourier transform infrared (FTIR) spectrometer consists of several vital components. The first component is an Infrared source such as a blackbody radiator or a globar, to produce a beam of IR radiation. The second component is the sample compartment, where the sample is placed for analysis. This sample may be in the form of a solid, liquid, or gas. The third component is the monochromator which is used to select a specific wavelength of IR radiation for analysis. It consists of a grating or prism that is used to disperse the IR radiation into its component wavelengths. The fourth component is a detector that measures the intensity of the transmitted or reflected IR radiation. The most common detectors in FTIR spectroscopy are thermal detectors, such as bolometers, and photodetectors, such as photodiodes or photomultiplier tubes. The fifth component is a data acquisition and analysis system which consists of a computer and software that are used to control the spectrometer, acquire and process the data, and display the results in the form of an absorbance or transmittance spectrum. The last component is the accessory components such as an attenuated total reflectance (ATR) accessory for analyzing solid samples, a liquid sample cell for analyzing liquid samples, or a gas cell for analyzing gases [31].

1.11 How FTIR Spectroscopy Works

A sample is placed in a sample compartment in the FTIR spectrometer. The sample can be in the form of a solid, liquid, or gas. Infrared radiation is generated by a light source, such as a globar or a tungsten-halogen lamp and is passed through the sample. The light source is usually coupled to a monochromator, which selects a specific range of wavelengths for the infrared radiation. As the infrared radiation passes through the sample, some of it is absorbed by the sample, while the rest is transmitted. The amount of infrared radiation absorbed by the sample depends on the chemical structure of the sample and the functional groups present. The absorbed infrared radiation is then detected by a mercury cadmium telluride (MCT) detector or

a pyroelectric detector. The detector generates an electrical signal proportional to the intensity of the absorbed infrared radiation. The resulting spectrum is plotted as a function of wavenumber (cm^{-1}), which measures the frequency of the infrared radiation. The resulting spectrum is a unique fingerprint of the sample and can be used to identify and analyze the sample's chemical composition. The absorption peaks in the spectrum correspond to specific vibrational modes of the functional groups present in the sample. The intensity and shape of these peaks can provide information about the chemical bonds and the structures of the molecules in the sample (Figure 1.9) [31].

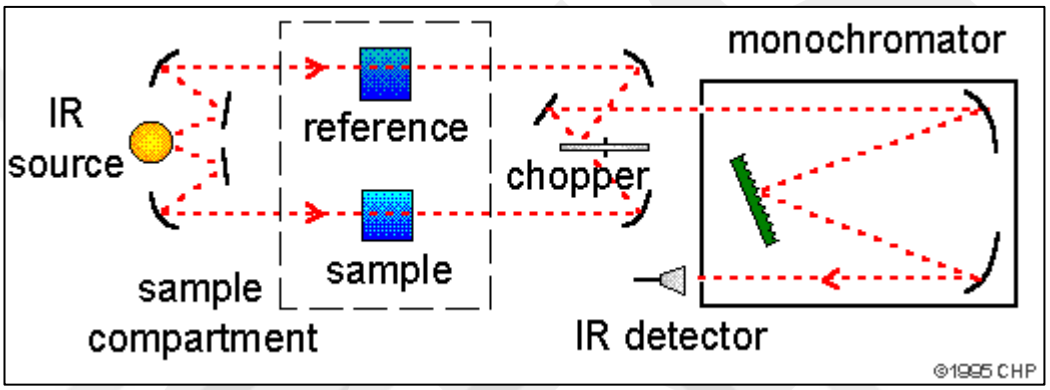

Figure 1.9 Simple FTIR spectroscopy diagram [33]

CHAPTER 2

MATERIALS AND METHODS

2.1 Materials

All chemicals used in this study are listed below (Table 2.1), all chemicals listed are used without additional purification.

Table 2.1 chemicals and instruments names used in this study

Compound name	Company name	Molecular weight	Chemical formula
Sodium Sulphate anhydrous	Aklar Kimya	142.04 g/mol	Na_2SO_4
Uric acid	SIGMA	168.11 g/mol	$C_5H_4N_4O_3$
Trisodium citrate dihydrate		294.10 g/mol	$Na_3C_6H_5O_7.2H_2O$
Creatinine anhydrous	Sigma Aldrich	113.12 g/mol	$C_4H_7N_2O$
Urea crystals	ISO LAB chemicals	60.06 g/mol	CH_4N_2O
Potassium chloride	Honeywell Riedel-de Haën	74.55 g/mol	KCl
Sodium chloride	Sigma Aldrich	58.44 g/mol	NaCl
Calcium chloride dihydrate	ISO LAB chemicals	147.01 g/mol	$CaCl_2.2H_2O$
Ammonium chloride	Tekkim	53.49 g/mol	NH_4Cl
Potassium Oxalate Monohydrate		166.22 g/mol	$K_2C_2O_4.H_2O$
Magnesium sulfate heptahydrate	Emir Kimya	246.48 g/mol	$MgSO_4.7H_2O$
Sodium dihydrogen phosphate dihydrate	Aklar Kimya	156.02 g/mol	$NaH_2PO_4.2H_2O$
Disodium hydrogen phosphate dihydrate	Aklar Kimya	177.99 g/mol	$Na_2HPO_4.2H_2O$

2.2 Artificial Urine Preparation

To prepare a normal multipurpose artificial urine (MP-AU), first, a glass beaker and a magnetic fish are cleaned with ethanol and distilled water. Then the magnetic fish is put in the glass beaker, and the beaker is filled with 100 ml of distilled water. The beaker with magnetic fish is placed on a magnetic stirrer with a heat plate (Heidolph MR Hei standard) to heat it to 37 ̊C to imitate the human body temperature. During this time, the chemicals used to prepare MP-AU are weighed using paper and a sensitive balance (OHAUS) with a sensitivity of 1×10^{-4}g. When distilled water reaches this temperature, the components of artificial urine are added in the same order shown in (Table 2.2). When all the analytes are added, the solution is left to stir at 37 ̊C for 10 minutes. At this point, it is an artificial urine solution with a specific gravity value of 1.015 and the pH value of 7. It is a colorless and odorless solution. After incubation, the solution is ready for spectroscopy investigation. The amount of each component of normal artificial urine, maximum amount and minimum amount used in this study is shown in (Table 2.2). The physiological range of components analytes of human urine is taken from [2]. The amount of each analyte that corresponds to the minimum, mid, and maximum value of the physiological range (Table 2.3).

Table 2.2 shows the amounts of chemical compounds used to prepare MP-AU

Average daily urine volume = 1.5 L							
	MW (g/mol)	**Physiological Range**	**Min (g/100ml)**	**Max (g/100ml)**	**Average (g/100ml)**	**N (mmol)**	**Molarity (mM)**
Urea	60.060	10-35 g/d	0.6	2.33	1.5	24.975	249.750
Uric acid	168.113	<750 mg/d	0	0.05	0.025	0.1487	1.487
Creatinine	113.120	Males: 955-2936 mg/d	0.06367	0.1957	0.1297	1.147	11.470
		Females: 601-1689 mg/d	0.0401	0.1126	0.0764	0.6754	6.754
Citrate	192.124	221-1191 mg/d	0.014733	0.0794	0.0470665	0.2449798	2.4497
Sodium	22.990	41-227 mmol/d	0.062839	0.3479	0.2054	8.9343	89.343
Potassium	39.098	17-77 mmol/d	0.04431	0.2007	0.1225	3.1332	31.332
Ammonium	18.050	15-56 mmol/d	0.01805	0.06739	0.04272	2.3668	23.668
Calcium	40.078	Males: <250 mg/d	0	0.0167	0.00835	0.2083	2083
		Females:<200 mg/d	0	0.01333	0.00667	0.16634	1663.42
Magnesium	24.305	51-269 mg/d	0.0034	0.01793	0.010665	0.43887	4388
Chloride	35.453	40-224 mmol/d	0.09454	0.52943	0.31199	8.8001	88001
Oxalate	88.018	0.11-0.46 mmol/d	0.00065	0.002699	0.001672	0.01897	187.73
sulphate	96.060	7-47 mmol/d	0.044828	0.300988	0.172908	1.8	18000

Table 2.3 chemicals used in the preparation of MP-AU

Compound	Minimum normal (g/100 ml)	MP-AU (g/100 ml)	Maximum normal (g/100 ml)
Sodium sulphate	0.0208	0.1700	0.3446
Uric acid	0	0.0250	0.0940
Trisodium citrate	0.0110	0.072	0.1490
Creatinine (women)	0.030	0.0881	0.211
Creatinine (men)	0.048	0.0881	0.367
Urea	0.5	1.5	3.750
Potassium chloride		0.2308	
Sodium chloride		0.1756	
Calcium chloride		0.0185	
Ammonium chloride		0.1266	
Potassium Oxalate Monohydrate		0.0035	
Magnesium sulphate	0.0132	0.1082	0.2194
Sodium dihydrogen phosphate	0.0739	0.2912	0.4621
Disodium hydrogen phosphate	0.0211	0.0831	0.1319

Minimum, maximum and average amounts of urea in MP-AU are calculated as an example as following:

First, the amount of minimum and maximum amount of urea is converted from g/1.5ml into g/100ml as follows:

$$minimum\ amount\ of\ urea = \frac{10g \times 100ml}{1500ml} = 0.67g/100ml \quad (2.1)$$

$$maximum\ amount\ of\ urea = \frac{35g \times 100ml}{1500ml} = 2.33g/100ml \quad (2.2)$$

The second step is calculating the average amount of urea as follows:

$$The\ average\ amount\ of\ urea = \frac{0.67+2.33}{2} = \frac{1.5g}{100ml} \quad (2.3)$$

The third step is calculating the number of moles in mM as follows:

$$no.of\ moles = \frac{weight\ in\ gram}{molecular\ weight} = \frac{1.5}{60.060} \times 10^3 = 24.975mmol \quad (2.4)$$

The last step is calculating the molarity as follows:

$$Molarity = \frac{number\ of\ moles\ in\ mM}{volume\ in\ liters} = \frac{24.975}{0.1} = 249.75\ mM \quad (2.5)$$

Five microliters from the prepared solution were taken and pipetted onto the diamond of the ATR. Then the spectrum of this sample is taken and visualized using the spectrometer software OMNIC. The previous step is repeated twice for the same solution, so each sample is scanned 3 times to measure the experimental error. In conclusion, 9 components were analyzed using 81 solutions.

2.3 ATR-FTIR Spectroscopy

The Nicolet 6700 (Thermo Scientific, USA) spectrometer is used to obtain the infrared absorbance spectrum. It has ten internal reflections in the form of a diamond Attenuated Total Refraction (ATR, ConcentratIR2, USA) accessory. A DTGS (Deuterated Tri Glycine Sulphate) detector is employed for each sample measurement, and a background interferogram is captured on a spotless diamond surface. A sample of 5ml is then pipetted onto the diamond and dried for 15 minutes using a moderate nitrogen stream. Drying the sample before data collection was preferred because water

absorption (H-O-H stretching) interacts with urea absorption. The drying period is maximized by drying the sample urine for 25 minutes and scanning it every 5 minutes. After 15 minutes, the O-H stretching vibration at 3400 cm^{-1} fades, and the amplitude of that region remains constant. In this manner, only the extra water is drained [24]. For a final resolution of 4 cm^{-1} on all samples, 120 scans are gathered and averaged. Actual points are separated by 0.96 cm^{-1}. The spectra are captured without using any techniques for digital signal augmentation. To remove ambient changes in water vapor during measurements, the interferometer's sample chamber is continually purged with N_2. Spectra's second derivative is computed using the Savitsky-Golay method with 17 smoothing points. Spectrometer software OMNIC version 8.2.388 is utilized to collect spectra and calculate derivatives (Thermo Scientific, USA).

2.4 Spectroscopic Analysis of Samples

First, the average of the three measurements was calculated to analyze these spectra. Three spectra are compared with the peak positions and heights for the spectral analysis of tested analytes. The first of the three spectra were obtained from the solution that included the minimum value of the physiological range for the tested analyte. The second of the three spectra were the MP-AU, in which all analytes are in mid-values. The last of the three spectra was obtained from the solution that included the maximum value of the physiological range for the tested analyte. Then each component is compared with its minimum spectrum. The peaks are followed from the x-axis and compared with peaks found in the spectrum of the component dissolved in distilled water. Using the literature information, peaks in the spectra correlate with molecular vibrations. Available functional groups were determined using the structure of the components. After the spectroscopic analysis of all spectra, they are transferred to Origin to generate pictures presented in this study. In the produced spectrum, the x-axis refers to the wavenumber of molecules, while the y-axis refers to the absorbance of the frequency by the molecules in the compound. The normal expectation is when the amount of the compound increases in the solution of MP-AU, the amplitude of the peaks increases as well as in peak 3430 cm^{-1} in the urea spectrum (Figure 2.1).

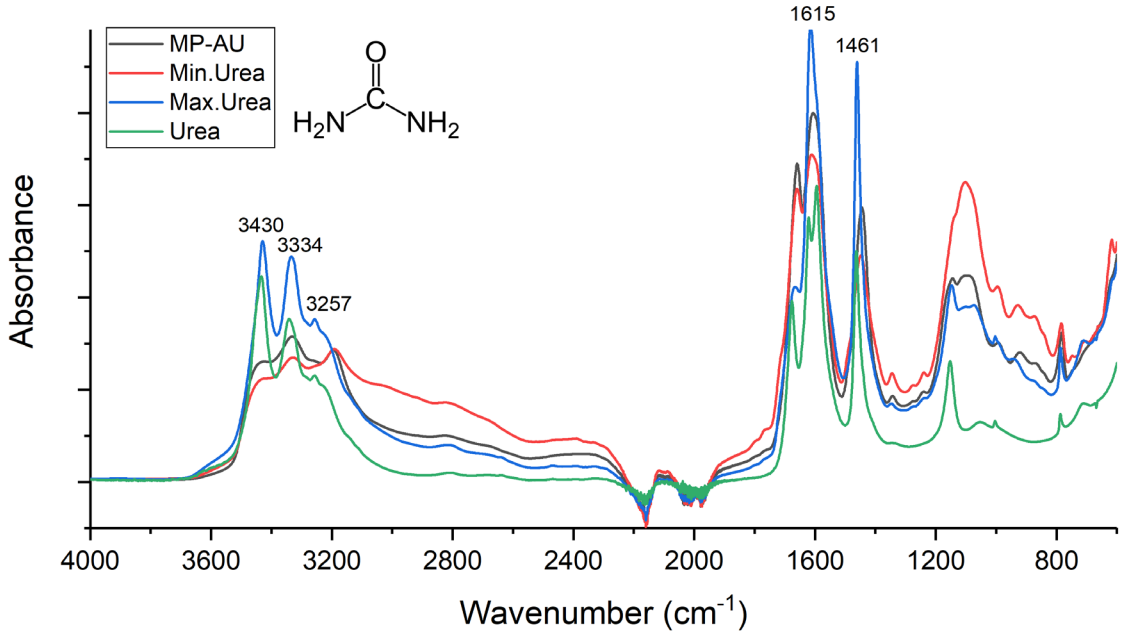

Figure 2.1 Urea spectrum as an example

CHAPTER 3

RESULTS AND DISCUSSION

An artificial urine solution is prepared and measured in triplets for each varying component. Three levels of magnitude were tested: minimum value of the normal range, mid-point of the normal range and maximum value of the normal range. The physiologically normal range of each substance is looked up on the Mayo Clinic website [2]. The change in the amount of a component from minimum to average and then to maximum can be followed by simultaneous changes in the FTIR spectra. This chapter presents all such spectra collected for each component, discusses the characteristic peaks of components, and attempts to correlate spectral peaks to vibrational modes in the structure of compounds.

3.1 Effect of Urea on MP-AU

In the high-frequency spectrum region, the range 3200-3500 cm^{-1} is affected dramatically by the changes in urea. The peak located at 3430 cm^{-1} grows in amplitude as the amount of urea changes from *a minimally normal* value to a *maximally normal* value in the mixture of MP-AU. The origin of this peak is the 3434 cm^{-1} urea peak that is obtained by scanning the urea only where this peak is due to NH_2 stretching vibrations. Also, the peak at 3334 cm^{-1} increases in amplitude as urea increases from *minimally normal* to *maximally normal* values. This peak is located at 3339 cm^{-1} in the urea spectrum. This peak is due to N-H stretching vibrations. Peak located at 3257 cm^{-1} grows in amplitude as the magnitude of urea increases from *a minimally normal* value to a *maximally normal* value. The origin of this peak is located at 3258 cm^{-1}, due to NH_2 stretching vibrations (Figure 3.1) [34].

In the low-frequency region, the peak located at 1615 cm^{-1} increases amplitude as urea increases from *minimally normal* to *maximally normal*. The position of this peak in the urea spectrum is located at 1621 cm^{-1}, due to C=O vibrations [34]. Another

peak at 1461 cm^{-1} grows in amplitude as urea increases from *minimally normal* to *maximally normal*. The origin of this peak is located at 1463 cm^{-1} in the urea spectrum, which is due to C-N vibrations (Figure 3.1) [34].

In the high-frequency region, the range 3179-2279 cm^{-1} decreases in amplitude as urea increases from minimally normal to maximally normal. Also, in the low-frequency region, the range 1898-1659 cm^{-1} and range 1345-619 cm^{-1} have an inverse relation with the magnitude of urea; as urea's magnitude increases, the amplitude decreases. This inverse action can be explained with a chemical reaction that clears these regions so that when more urea is added to the solution, there is more reaction with an already existing urine component, which is then relocated (Figure 3.1).

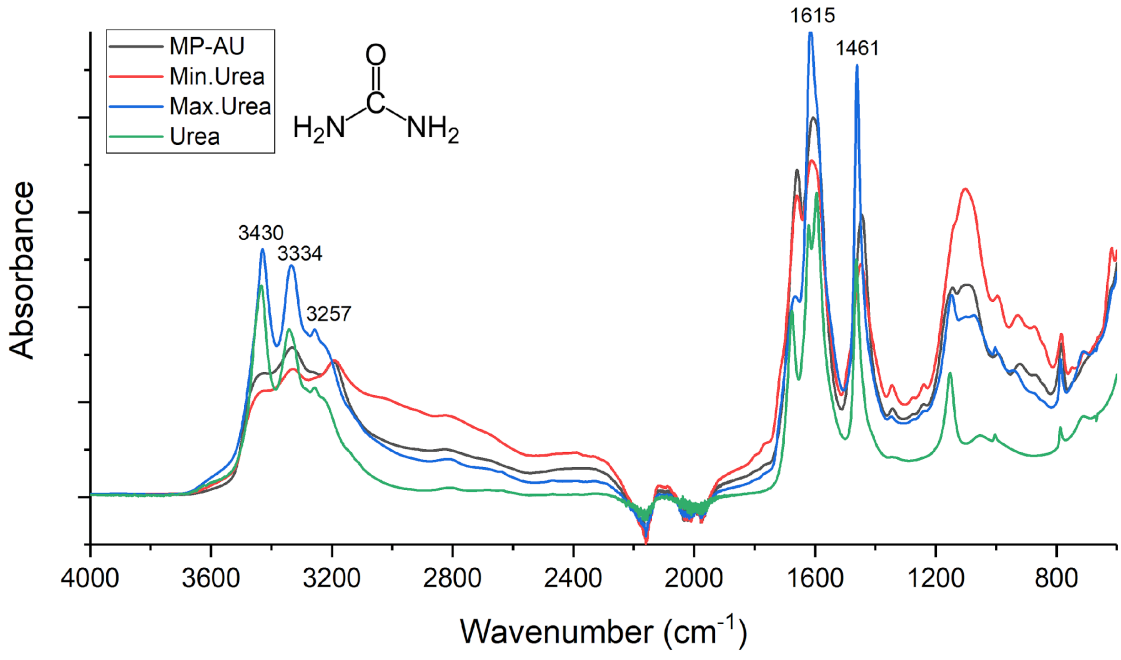

Figure 3.1 The infrared spectrum of MP-AU (black), MP-AU with the minimum amount of urea (red), MP-AU with the maximum amount of urea (blue) and urea in distilled water

3.2 Effect of Glucose on MP-AU

In the high-frequency region in the range of 3000-3500 cm^{-1}, the amplitude is directly proportional to the magnitude of glucose. Amplitude increases as glucose

increases in MP-AU from *a minimally normal* value to *a maximally normal* value. Comparing this range with the spectrum of glucose in distilled water in the same region, a broad hump is seen. So this increasing peak is due to one of the functional groups of glucose. The suggested functional group is the O-H stretching vibrations (Figure 3.2) [34].

In the low-frequency region, there is a slight change at the position 993 cm^{-1}, where the amplitude decreases as the glucose amount increases from *minimally normal* to *maximally normal* value. Looking at the spectrum of glucose, there is a peak located at 1024 cm^{-1}, which might explain the amplitude change at 993 cm^{-1}. This peak is assigned to the C-O vibrations in the structure of glucose (Figure 3.2) [34].

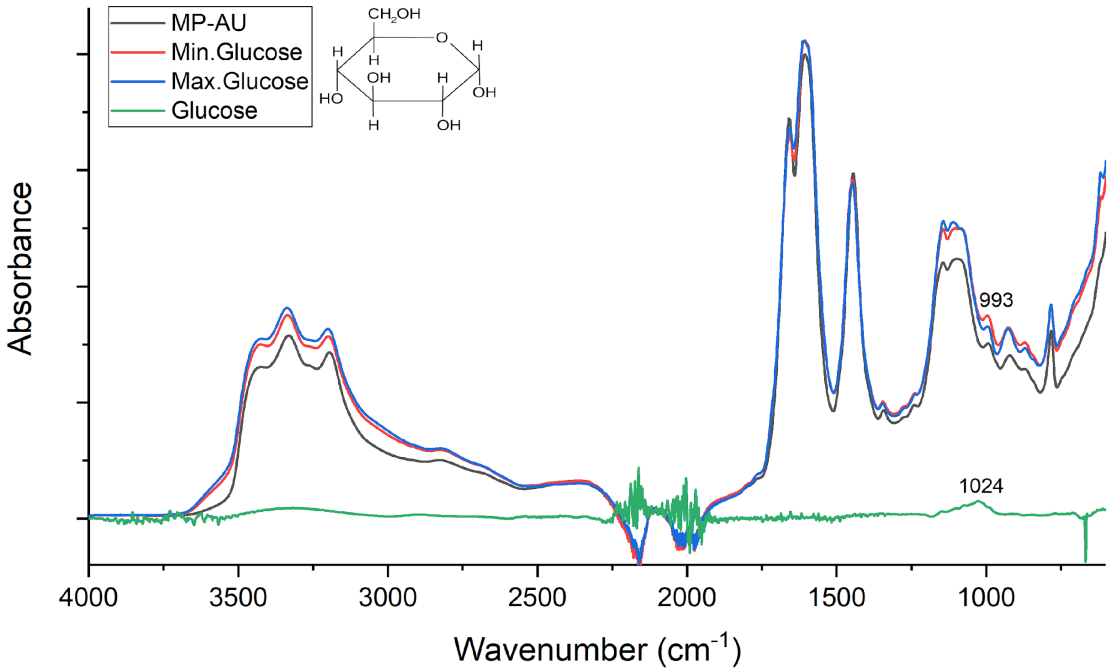

Figure 3.2 Shows the full FTIR spectrum of MP-AU (black), MP-AU with the minimum amount of glucose (red), MP-AU with the maximum amount of glucose (blue) and glucose in distilled water (green)

3.3 Effect of Creatinine on MP-AU Formulated for Women

There is a big difference between the spectrum of creatinine in MP-AU of women and that of men. This difference is due to the variation in the magnitude of

maximum and minimum creatinine in MP-AU between men and women. The minimum amount of creatinine in MP-AU of men is 0.048 g/100ml, and that of women is 0.030 g/100ml. On the other hand, the maximum creatinine value for men is 0.367 g/100ml, while for women is 0.211 g/100ml. So as there is more amount of creatinine in men, there are more interactions between creatinine and other components in MP-AU.

In the high-frequency region, creatinine causes several changes simultaneously as the amount of creatinine increases from *minimally normal* to *maximally normal*. For example, the amplitude of peaks at 3430 cm^{-1} and 3332 cm^{-1} decrease as the magnitude of creatinine increases from *the minimally normal* value in MP-AU to the *maximally normal* value. This inverse relationship can be due to an indirect reaction between creatinine and other urine components used in the formulation of MP-AU. This suggested component in urine is urea. The origin region of these two peaks in the creatinine spectrum is due to O-H vibrations [34]. The peak amplitude located at 3256 cm^{-1} decreases as the amount of creatinine in MP-AU increases from *minimally normal* to *maximally normal*. The normal position of this peak in the creatinine spectrum is at 3247 cm^{-1}, which is due to N-H stretching vibrations [34]. The peak located at 2805 cm^{-1} decreases in amplitude as the magnitude of creatinine increases in MP-AU. The origin position of this peak is located at 2802 cm^{-1} in the creatinine spectrum, which is due to the CH_3 group found in the creatinine structure (Figure 3.3) [34].

In the low-frequency region, peaks at 1659 cm^{-1}, 1342 cm^{-1} and 1242 cm^{-1} grow in amplitude as the magnitude of creatinine increases in MP-AU from *minimally normal* to *maximally normal*. The origin of these peaks is located at 1666 cm^{-1}, 1330 cm^{-1} and 1244 cm^{-1}, respectively, in the spectrum of creatinine. These peaks are due to C=O stretching vibrations, C-N stretching vibrations and CNH vibrations [34]. Peaks located at 1615 cm^{-1} and 1461 cm^{-1} are shifted, and their amplitude decreases as the magnitude of creatinine increases from *minimally normal* to *maximally normal*. Range 1060-869 cm^{-1} decrease in amplitude as the magnitude of creatinine increases from *minimally normal* to *maximally normal* (Figure 3.3).

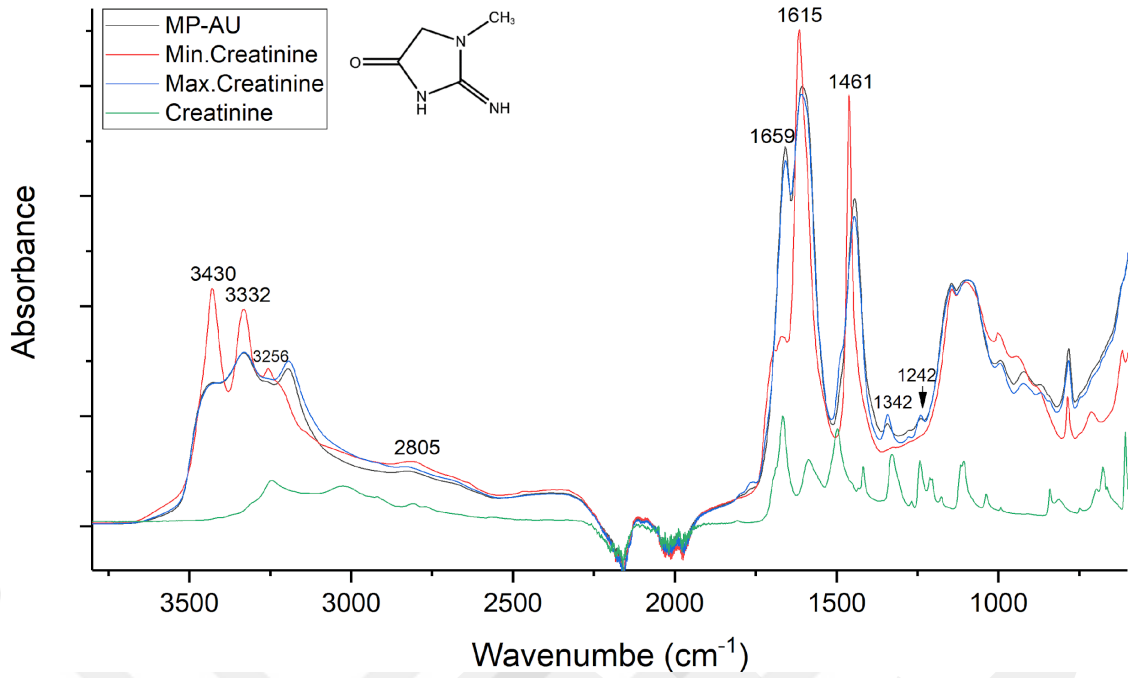

Figure 3.3 The infrared spectrum of MP-AU (black), MP-AU with the minimum amount of creatinine (red), MP-AU with the maximum amount of creatinine (blue) and creatinine in distilled water (green)

3.4 Effect of Creatinine on MP-AU Formulated for Men

In the high-frequency region, there are two peaks at 3428 cm^{-1} and 3335 cm^{-1} that decrease in amplitude as the amount of creatinine increases from *minimally normal* to *maximally normal.* This inverse relationship can be due to an indirect reaction between creatinine and urea, which is used in the formulation of MP-AU. The only peak in the same region in the creatinine spectrum is at 3248 cm^{-1} due to N-H vibrations [34]. Range 3248-2924 cm^{-1} increases in amplitude as the magnitude of creatinine increases from minimally normal to maximally normal values in MP-AU. At the same range in the creatinine spectrum, a wide hump is seen. This hump is due to C-H stretching vibrations (Figure 3.4) [34].

In the low-frequency region, the peak located at 1487 cm^{-1} increases in amplitude as the amount of creatinine increases from *minimally normal* to *maximally normal*. The normal position of this peak is located at 1498 cm^{-1} in the creatinine spectrum. This peak is due to CH_3 deformation [34]. Peak located at 1342 cm^{-1} increases in amplitude as the amount of creatinine increases from *a minimally normal* value to a

maximally normal value in MP-AU. The origin of this peak is located at 1330 cm^{-1} in the creatinine spectrum. This peak is due to C-N stretching vibrations found in the structure of creatinine [34]. Peak located at 1243 cm^{-1} increases in amplitude as the magnitude of creatinine increases in MP-AU from *minimally normal* to *maximally normal*. The origin peak is located at the same position in the creatinine spectrum due to CNH vibrations [34]. Peak located at 842 cm^{-1} grows in amplitude as the creatinine increases from *minimally normal* to *maximally normal*. The origin peak is located at the same position in the creatinine spectrum due to N-CH_3 vibrations in the structure of creatinine (Figure 3.4) [34].

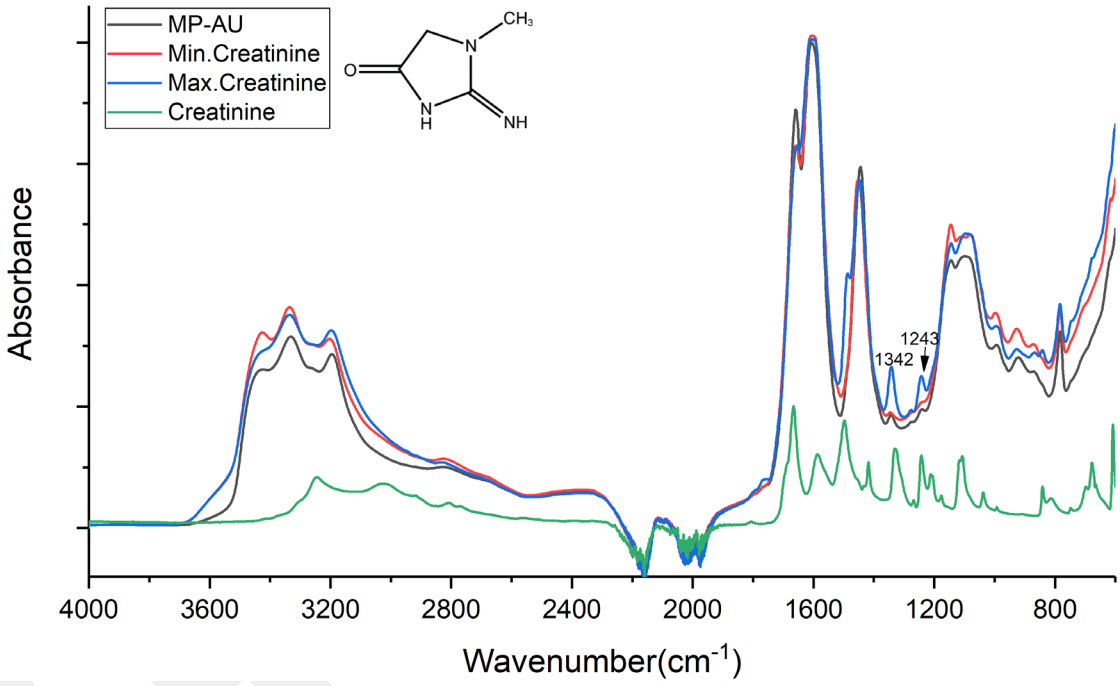

Figure 3.4 The infrared spectrum of MP-AU (black), MP-AU with the minimum amount of creatinine (red), MP-AU with the maximum amount of creatinine (blue) and creatinine in distilled water (green)

3.5 Effect of Sodium Phosphate on MP-AU

In the high-frequency region, the range 3518-3144 cm^{-1} decreases in amplitude as the amount of sodium phosphate increases in MP-AU from minimum normal value to maximum normal value. A large hump in the sodium phosphate spectrum is in the same range due to OH stretching vibrations [34]. This inverse relation between the amplitude of MP-AU and the amount of sodium phosphate may be due to the interaction between sodium phosphate and another component of MP-AU, and the suggested component is urea. Range 3144-2328 cm^{-1} increases in amplitude as the amount of sodium phosphate increases in MP-AU from minimum normal value to maximum normal value. There is a broad hump at the same range in the sodium phosphate spectrum, and it is due to OH stretching vibrations of the P-OH group (Figure 3.5) [34].

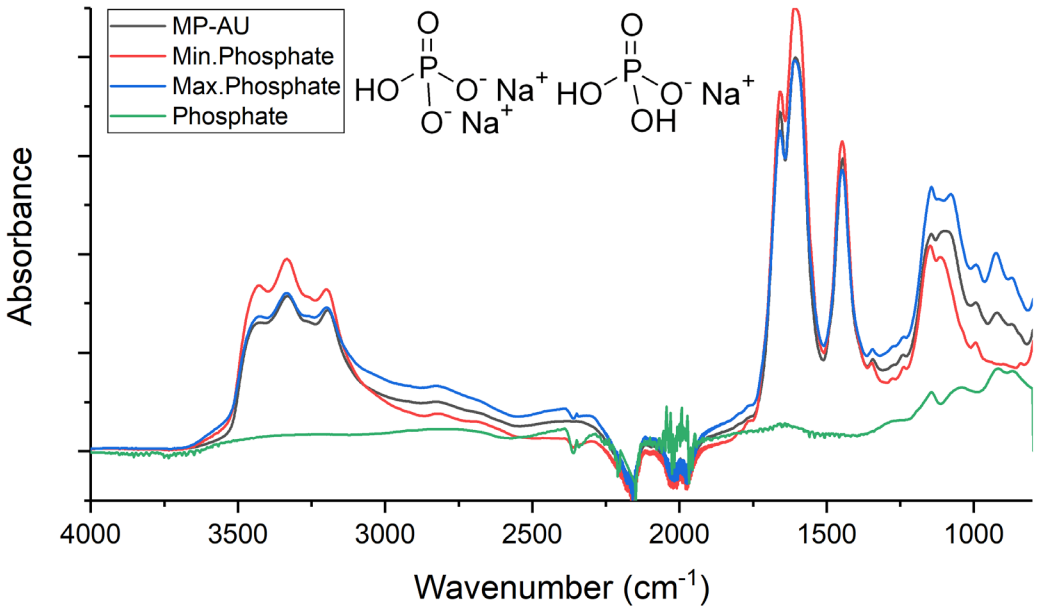

Figure 3.5 FTIR spectra of MP-AU (black), MP-AU with the minimum amount of sodium phosphate (red), MP-AU with the maximum amount of sodium phosphate (blue), Di-sodium hydrogen phosphate in distilled water (green) and sodium dihydrogen phosphate in distilled water

In the low-frequency region, peaks located at 1658 cm^{-1}, 1603 cm^{-1} and 1448 cm^{-1} decrease in amplitude with increases in the amount of sodium phosphate in MP-AU from minimum normal value to maximum normal value. A band in the sodium phosphate spectrum is in the same range due to HO-P=O vibrations. So, this inverse relationship may be due to the interaction between sodium phosphate and urea in MP-AU [34]. Peak located at 1144 cm^{-1} grows in amplitude as the magnitude of phosphate increases from minimum normal value to maximum normal value in MP-AU. There is a peak at 1145 cm^{-1} in the sodium phosphate spectrum due to P=O stretching vibrations (page 364). Another peak at 1076 cm^{-1} increases in amplitude as sodium phosphate's amount increases from the minimum value to the maximum value. The normal position of this peak in the sodium phosphate spectrum is located at 1075 cm^{-1} due to PO_2^- stretching vibrations [34]. Peaks at 990 cm^{-1},924 cm^{-1},867 cm^{-1}, and 783 cm^{-1} increase in amplitude as the amount of sodium phosphate increases from minimum normal value to maximum normal value. The reason for these peaks is P-O-P stretching vibrations found at the range 1000-800 cm^{-1} in the sodium phosphate spectrum (Figure 3.5) [34].

3.6 Effect of Sodium Citrate on MP-AU

In the high-frequency region, the range 3481-2968 cm^{-1} has an inverse relation in amplitude with the magnitude of sodium citrate. The amplitude decreases as sodium citrate increases in MP-AU from *minimally normal* to *maximally normal*. This inverse relationship can be due to an indirect reaction between sodium citrate and other components of MP-AU. One of the suggested components is urea. At the same range in the sodium citrate spectrum, a large hump is visible. This hump is due to OH stretching vibrations (Figure 3.6) [34].

In the low-frequency region, the peak located at 1605 cm^{-1} increases in amplitude as sodium citrate increases from *minimally normal* to *maximally normal*. At the same region in the sodium citrate spectrum, a peak located at 1572 cm^{-1} appears. This peak is due to COO^- stretching vibrations found in the structure of sodium citrate [34]. Range 1457-1318 cm^{-1} increases amplitude as the amount of sodium citrate increases in MP-AU from minimum normal to maximum normal value. In addition, there is a

peak at 1391 cm^{-1} in the sodium citrate spectrum due to COH vibrations (Figure 3.6) [34] .

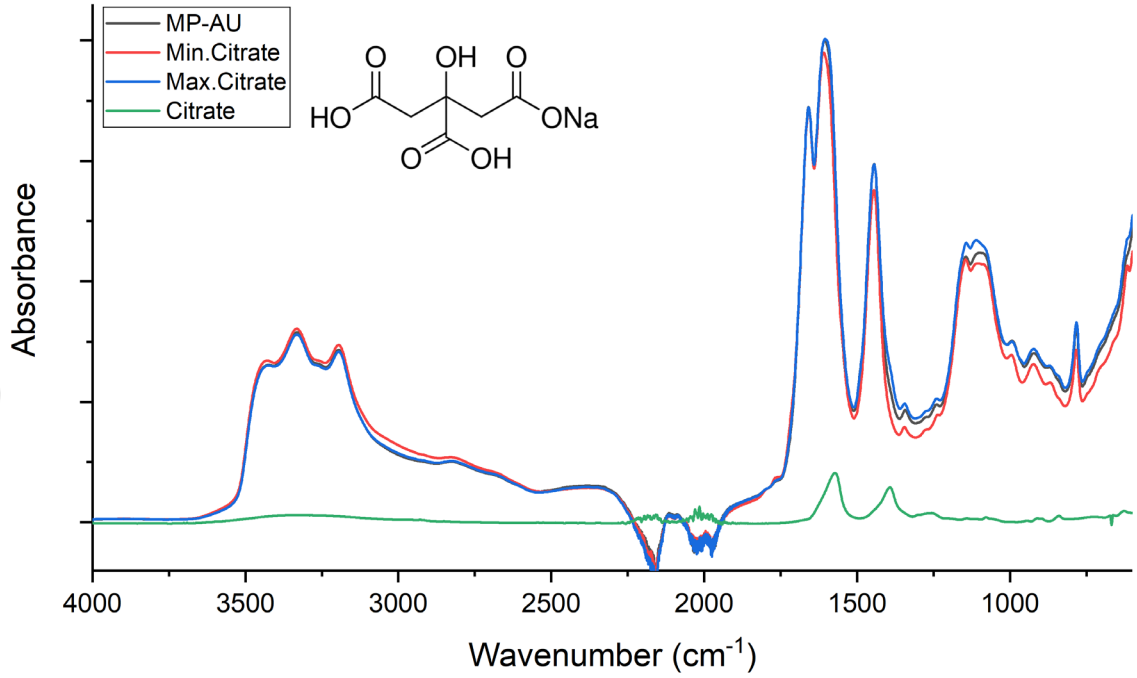

Figure 3.6 shows spectra of MP-AU (black), MP-AU with the minimum amount of citrate (red), MP-AU with the maximum amount of citrate (blue) and citrate in distilled water (green)

3.7 Effect of Sulphate on MP-AU

In the high-frequency region, the peaks located at 3425 cm^{-1} and 3335 cm^{-1} increase in amplitude as the magnitude of Sulphate increases from *minimally normal* to *maximally normal*. The origin of these two peaks is a wide absorption at the range 3600-3000 cm^{-1} in the sulphate spectrum due to O-H vibrations caused when Sulphate interacts with water molecules in the solution [34]. The range 3204-2324 cm^{-1} decreases in amplitude as the magnitude of sulphate increases from *minimally normal* to *maximally normal* (Figure 3.7).

In the low-frequency region, the peaks located at 1659 cm^{-1} and 1607 cm^{-1} decrease in amplitude as the amount of sulphate increases in MP-AU from the minimum value to the maximum value. In the same region, the sulphate spectrum

shows a band range of 1700-1652 cm^{-1} due to OH bending vibrations [34]. The peak at 1148 cm^{-1} grows in amplitude as the amount of sulphate increases in MP-AU from minimally normal to maximally normal. The underlying peak at 1140 cm^{-1} in the sulphate spectrum is due to SO_2^- stretching vibrations [34]. Peak located at 1094 cm^{-1} increases in amplitude as the magnitude of Sulphate increases from minimum normal value to maximum normal value. The original peak is located at 1098 cm^{-1} in the sulphate spectrum due to SO_4 stretching vibrations [34]. Another peak at 1077 cm^{-1} grows in amplitude as the magnitude of sulphate increases in MP-AU from minimum normal to maximum normal value. The position of this peak is located at 1075 cm^{-1} in the sulphate spectrum, and it is due to S=O stretching vibrations [34]. Peak located at 994 cm^{-1} increases in amplitude as the amount of Sulphate increases from minimum normal value to maximum normal value. At the same location in the sulphate spectrum, there is a peak due to in-phase SO_4 stretching vibrations [34]. In the minimum normal spectrum, there is a peak located at 927 cm^{-1}, which disappears in the maximum normal spectrum, most probably due to an interaction with another component of MP-AU. The suggested component is sodium phosphate (Figure 3.7).

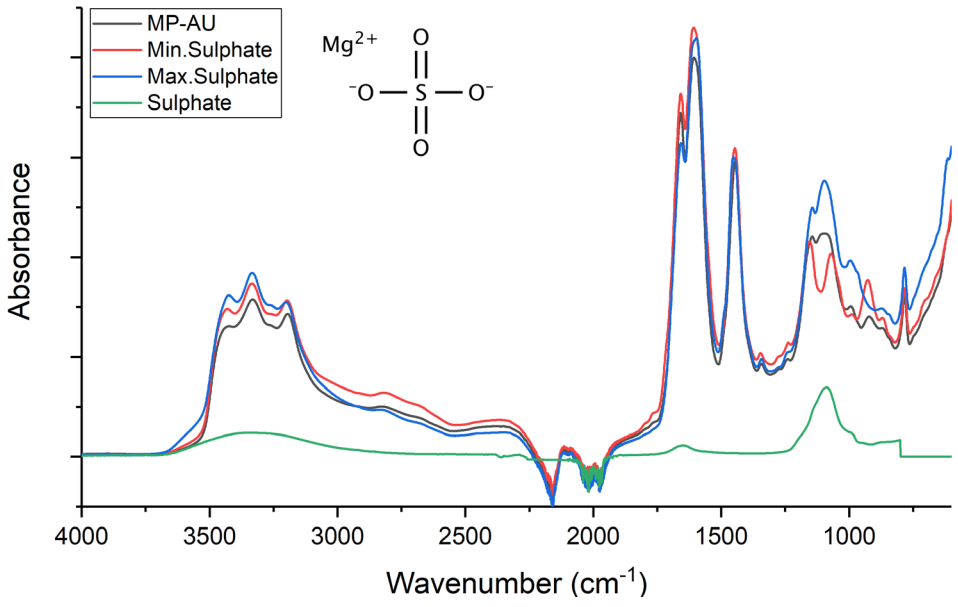

Figure 3.7 The infrared spectrum of MP-AU (black), MP-AU with minimum amount of Sulphate (red), MP-AU with maximum amount of Sulphate (blue) and Sulphate multiplied by 3 in distilled water (green)

3.8 Effect of Albumin on MP-AU

In the high-frequency regions, peaks at 3435 cm^{-1}, 3335 cm^{-1} and 3199 cm^{-1} grow in amplitude as the magnitude of albumin increases in MP-AU from minimally normal to maximally normal. There is a peak located at 3294 cm^{-1} in the spectrum of albumin in distilled water, and this peak is due to N-H stretching vibrations (Amide A) found in the structure of albumin (Figure 3.8) [35].

In the low-frequency region, peaks located at 1659 cm^{-1}, 1602 cm^{-1} and 1445 cm^{-1} decrease in amplitude as the amount of albumin increases from minimally normal to maximally normal. At the same region in the albumin spectrum, peaks located at 1653 cm^{-1} and 1540 cm^{-1} refer to C=O stretching vibrations (Amide I) and N-H bending vibrations (Amide II), which are found in the structure of albumin (Figure 3.8) [35].

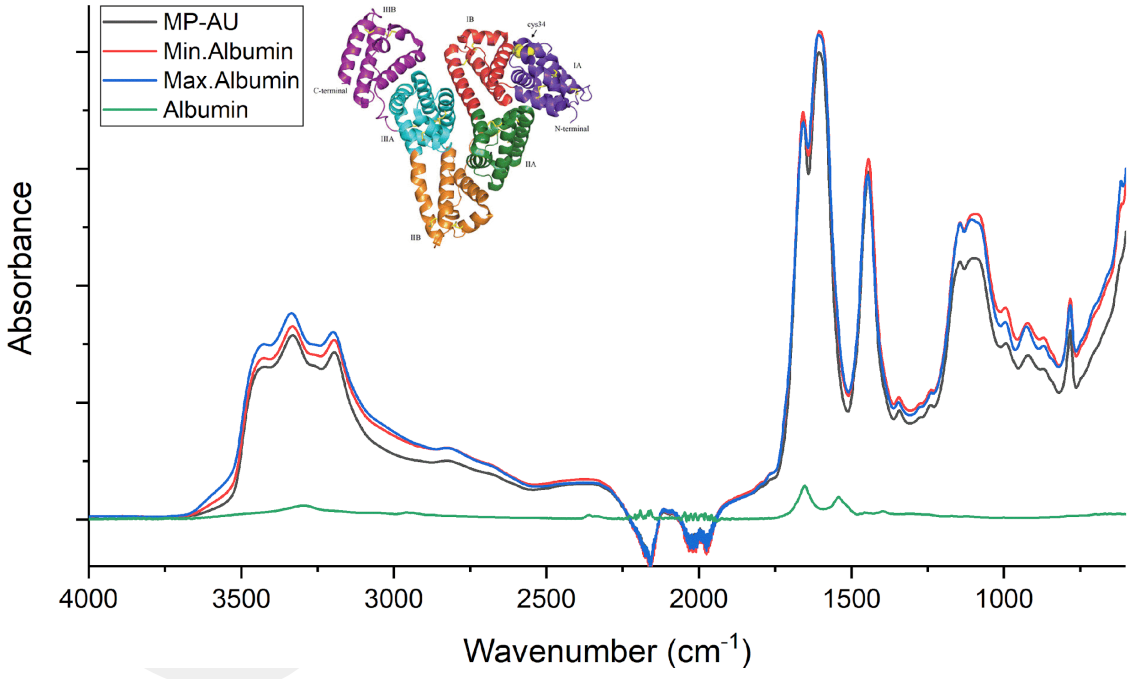

Figure 3.8 spectrum of MP-AU (black), MP-AU with the minimum amount of albumin (red), MP-AU with the maximum amount of albumin (blue) and albumin in distilled water (green), source of Image of albumin [36]

3.9 Effect of Uric Acid on MP-AU

In the high-frequency region, the range 3416-2541 cm^{-1} increases in amplitude as the amount of uric acid increases from minimum normal value to maximum normal value in MP-AU. However, at the same region in the uric acid spectrum, there is a wide hump due to OH stretching vibrations (Figure 3.9) [34]. In the low-frequency regions, the peak located at 1655 cm^{-1} increases in amplitude as the magnitude of uric acid increases from the minimum normal value to the maximum normal value in MP-AU. The origin of this peak is located at 1658 cm^{-1} in the uric acid spectrum due to C=O stretching vibrations (page 390). Peak located at 1598 cm^{-1} increases in amplitude as the amount of uric acid increases from minimum normal to maximum normal value. The origin of this peak is located at 1582 cm^{-1} in the uric acid spectrum due to CN stretching vibrations [34]. Another peak at 1341 cm^{-1} grows in amplitude as the magnitude of uric acid increases in MP-AU from minimum normal to maximum normal value. The origin of this peak is located at 1346 cm^{-1} in the spectrum of uric acid, which is due to C=O vibrations [34]. Peaks located at 1117 cm^{-1}, 990 cm^{-1}, 872 cm^{-1} and 758 cm^{-1} increase in amplitude as the magnitude of uric acid increases from minimum normal value to maximum normal value in MP-AU. The normal positions of these peaks are visible in the spectrum of uric acid at 1120 cm^{-1}, 90 cm^{-1}, 875 cm^{-1} and 782 cm^{-1}, respectively. The reason for these peaks is C-O stretching vibrations (Figure 3.9) [34].

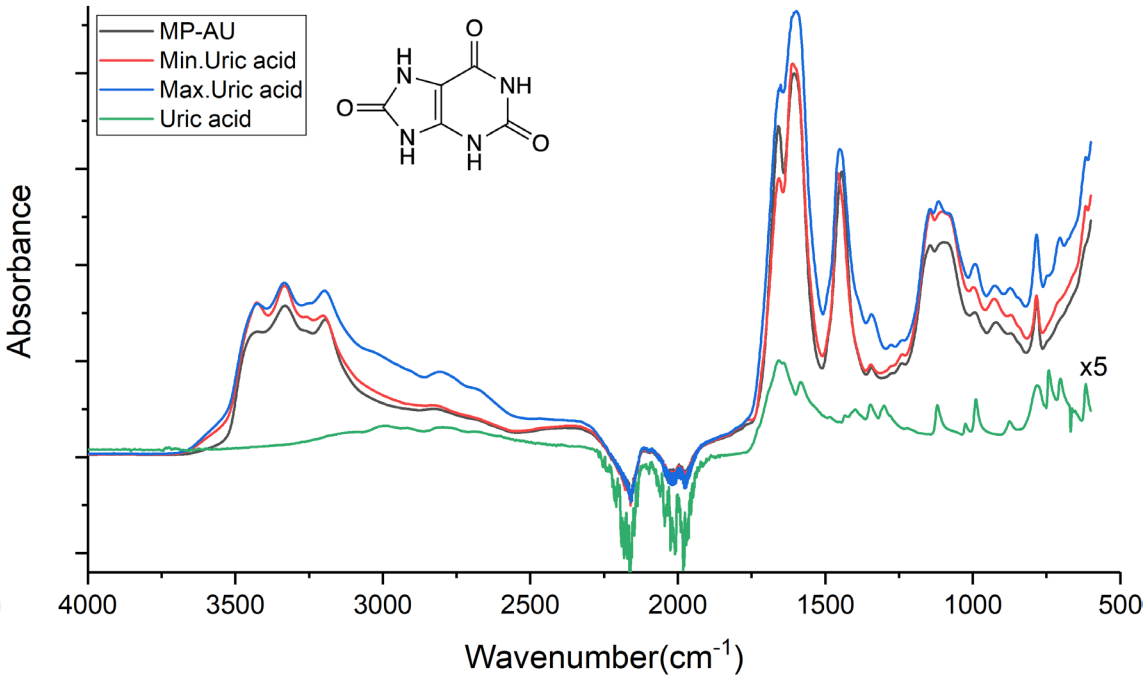

Figure 3.9 Spectra of MP-AU (black), MP-AU with the minimum amount of uric acid (red), MP-AU with the maximum amount of uric acid (blue) and uric acid in distilled water magnified by five times (green)

Instead of changing the urine components in magnitude one by one, all components were also used in the minimum amount in the same artificial urine solution to construct a spectral image of a normal urine in the lower limit of the physiological range (Figure 3.10-red). Alternatively, all components were used in the maximum possible amount to construct another spectral image of a normal urine in the upper limit of the physiological range (Figure 3.10-blue). These two spectra can be considered as drawing the limits of "spectral normal" of any urine spectrum. The region 1500-1000 cm^{-1} is seen to change between these two spectra. This is expected because most of the components tested in this study have a signature band directly or have an indirect effect on this region. Therefore, this region is expected to show the greatest variation among healthy human urine samples.

A previous study by Sarigul, et al. (2022) showed that healthy human urine samples show variations in the same region even for the same age groups (Figure 3.11). This result is in accordance with the data obtained in this study. Variations seen in other regions depend on the age group of the sample. In adults (Figure 3.11-C), 1800-

1200 cm^{-1} region is variable, showing differences among individuals. This region is mainly characterized by changes in urea, which depends mostly on the diet. In the artificial system, the same region is also seen to be greatly affected by changes in urea. Thus, data obtained in this study regarding the natural urine components and their contribution to urine spectra can be used for pre-screening of urine samples together with biochemical assays.

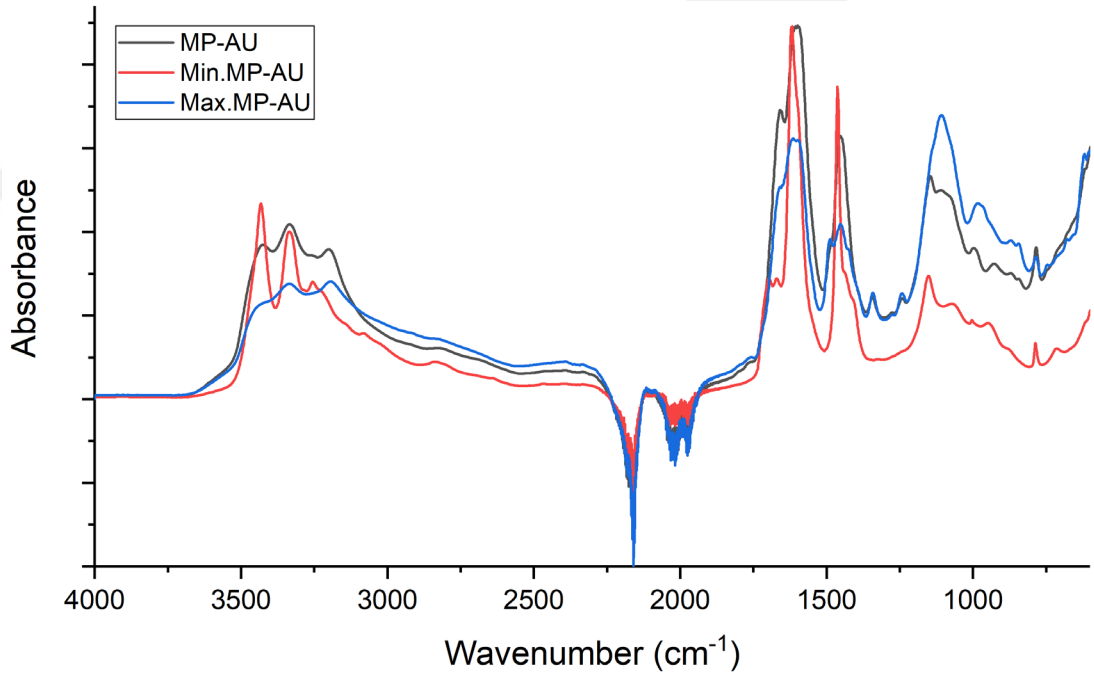

Figure 3.10 The average spectrum of MP-AU (black), MP-AU with the minimum amount of all components (red), MP-AU with the maximum amount of all components (blue)

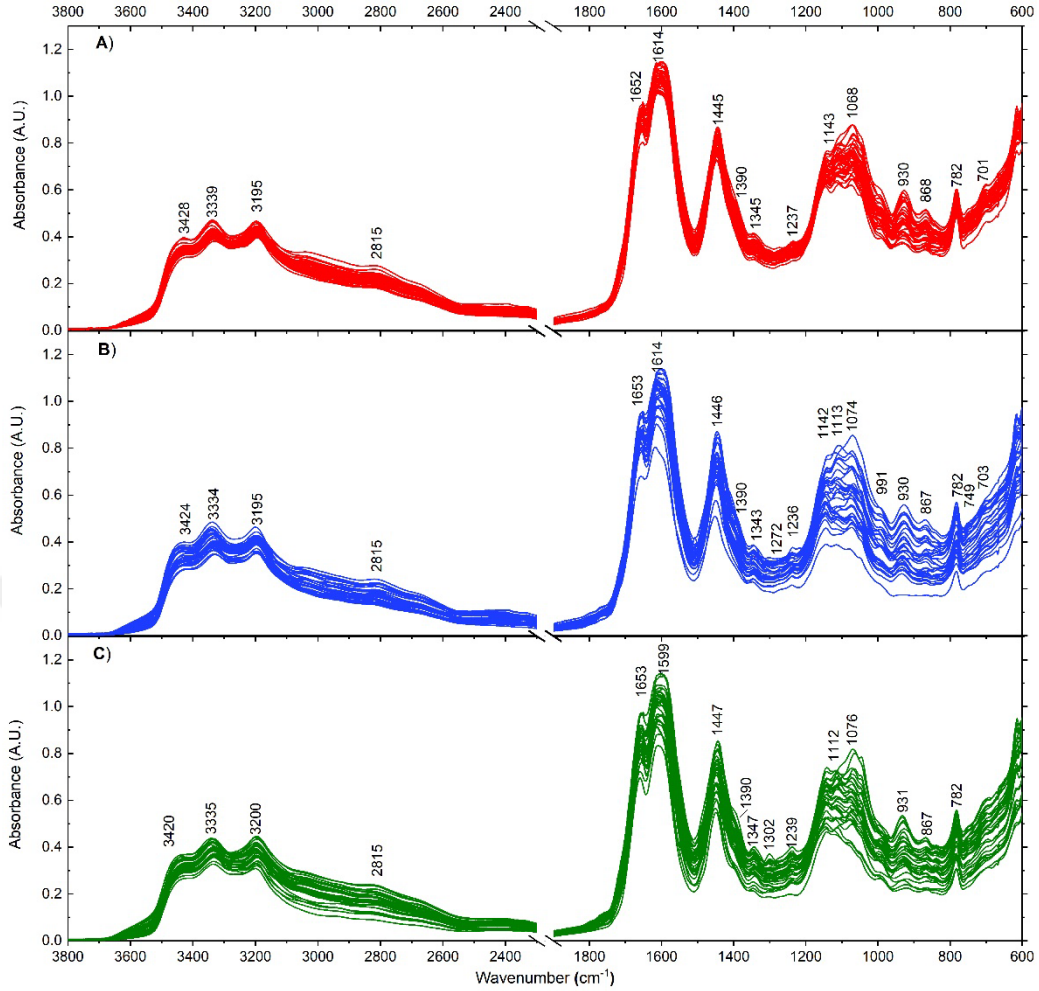

Figure 3.11 Human urines taken from different volunteers of different ages; A: children aged 3 to 10, B: young adults aged 20 to 30, C: adults aged 31 to 40. (Figure taken from Sarigul et al., 2022 with the permission of authors)

CHAPTER 4

CONCLUSION

Human urine is a vital fluid as it carries information about systemic and urinary tract health. In previous research, a new protocol for an artificial urine solution was produced that mimics healthy urine samples in terms of spectroscopic properties. Using this new protocol, this study attempted to find the maximum normal, the minimum normal and the average of a healthy human urine. FTIR spectroscopy was used to obtain the spectra of 8 urine components changing in MP-AU from minimum normal to maximum normal value. These components are sulphate, urea, creatinine, albumin, glucose, citrate, uric acid and phosphate. For each component, the spectrum of maximum normal value was compared with that of the minimum normal value and with the spectrum of the component dissolved in distilled water.

The most effective components that change the spectra in the high frequency region are urea and uric acid. The spectral changes in the region above 3300 cm^{-1} are due to urea, while in under this region are due to uric acid. On the other hand, the most effective components in the low-frequency region are urea, phosphate, citrate, sulphate, and uric acid.

In the high frequency region, increasing some components from minimum normal value to maximum normal value gives an inverse relationship between the amplitude and the magnitude. It is visible that amplitude decreases when magnitude increases from minimum normal value to maximum normal value. These components are citrate, creatinine and phosphate. This inverse relation is due to the interaction between these components and another component of MP-AU. The suggested component is the urea as it contains hydrogen, which can interact with the free oxygen in the previous components. On the other hand, three components give the inverse relationship between the components' amplitude and magnitude in the low-frequency region. These components are urea, creatinine (in the case of women), and phosphate.

So, this study can help in diagnosing patients by looking for their spectra and comparing them with a spectrum of the normal range. For example, if the spectrum of the patient is between the normal maximum and normal minimum, the patient can be considered healthy. Likewise, if the spectrum of the patient is above or under this range, this implies that the patient can have a health problem.

REFERENCES

[1] S. Bouatra *et al.*, "The Human Urine Metabolome," *PLOS ONE,* vol. 8, no. 9, p. e73076, September 2013.

[2] N. Sarigul, F. Korkmaz, and I. Kurultak, "A New Artificial Urine Protocol to Better Imitate Human Urine," *Scientific Reports,* vol. 9, no. 1, December 2019, 6, 9.

[3] H. Maurya, T. Kumar, and S. Kumar, "Anatomical and Physiological Similarities of Kidney in Different Experimental Animals Used for Basic Studies," *Journal of Clinical & Experimental Nephrology,* vol. 03, no. 2, 9, pp. 1-6, 2018.

[4] M. D. MD, "Kidney Anatomy." https://step1.medbullets.com/renal/115001/kidney-anatomy, Nov. 5, 2022 [Dec. 1, 2022].

[5] H. W. Smith, H. Chasis, W. P. D. Goldring, and H. A. Ranges, "Glomerular Dynamics in the Normal Human Kidney," *The Journal of clinical investigation,* vol. 19, no. 5, pp. 751-64, 1940.

[6] R. J. Leatherby, C. Theodorou, and R. Dhanda, "Renal Physiology: blood flow, glomerular filtration and plasma clearance," *Anaesthesia & Intensive Care Medicine,* vol. 22, no. 7, pp. 439-42, July 2021.

[7] V. Vallon, "Tubuloglomerular Feedback and the Control of Glomerular Filtration Rate," *Physiology,* vol. 18, no. 4, pp. 169-74, August 2003.

[8] V. Vallon and S. C. Thomson, "The Tubular Hypothesis of Nephron Filtration and Diabetic Kidney Disease," *Nature Reviews Nephrology,* vol. 16, no. 6, pp. 317-36, June 2020.

[9] Eden, "Breaking Down Nephron Functioning Into Six Easy Steps." https://blog.cambridgecoaching.com/a-comprehensive-break-down-of-nephron-functioning-into-six-easy-steps, [Dec. 12, 2022].

[10] R. L. Lammers, S. C. Gibson, D. Kovács, W. N. Sears, and G. Strachan, "Comparison of Test Characteristics of Urine Dipstick and Urinalysis at Various Test Cutoff Points," *Annals of emergency medicine,* vol. 38, no. 5, pp. 505-12, November 2001.

[11] J. R. Raymond and W. E. Yarger, "Abnormal Urine Color: Differential Diagnosis," *Southern Medical Journal,* vol. 81, no. 7, pp. 837-41, July 1988.

[12] C. C. Mbonu, O. Kilanko, M. B. Kilanko, and P. O. Babalola, "Turbidity and Urine Turbidity: A Mini Review," in *Bioenergy and Biochemical Processing Technologies: Recent Advances and Future Demands*, A. O. Ayeni, S. E.

Sanni, and S. U. Oranusi Eds. Cham: Springer International Publishing, 2022, pp. 253-67.

[13] J. A. Simerville, W. C. Maxted, and J. J. Pahira, "Urinalysis: A Comprehensive Review," (in eng), *American family physician,* vol. 71, no. 6, pp. 1153-62, March 2005.

[14] G. B. Fogazzi and G. Garigali, "The Clinical Art and Science of Urine Microscopy," (in eng), *Current opinion in nephrology and hypertension,* vol. 12, no. 6, pp. 625-32, November 2003.

[15] C. Pollock *et al.*, "Dysmorphism of Urinary Red Blood Cells--Value in Diagnosis," (in eng), *Kidney International,* vol. 36, no. 6, pp. 1045-9, December 1989.

[16] P. Lamchiagdhase *et al.*, "Urine Sediment Examination: A Comparison Between the Manual Method and the iQ200 Automated Urine Microscopy Analyzer," *Clinica Chimica Acta,* vol. 358, no. 1-2, pp. 167-74, August 2005.

[17] D. Vickers, T. Ahmad, and M. G. Coulthard, "Diagnosis of urinary tract infection in children: fresh urine microscopy or culture?," *The Lancet,* vol. 338, no. 8770, pp. 767-70, September 1991.

[18] S. R. Khan and R. L. Hackett, "Identification of Urinary Stone and Sediment Crystals by Scanning Electron Microscopy and X-Ray Microanalysis," *Journal of Urology,* vol. 135, no. 4, pp. 818-25, April 1986.

[19] Y. M. Fazil Marickar, P. R. Lekshmi, L. Varma, and P. Koshy, "Elemental Distribution Analysis of Urinary Crystals," (in eng), *Urological Research,* vol. 37, no. 5, pp. 277-82, October 2009.

[20] R. Bhutta, N. Syed, A. Ahmad, and S. Khan, "Urine Analysis." https://labpedia.net/category/lab-tests/urine-analysis, [Dec. 26, 2022].

[21] D. W. Ball, "The Electromagnetic Spectrum: A History," *Spectroscopy,* vol. 22, no. 3, pp. 14-20, March 2007.

[22] J. Lambert, R. Bleicher, B. Soden, A. Edwards, and A. Henderson, "Electromagnetic Radiation." http://www.ces.fau.edu/nasa/module-2/radiation-sun.php, Oct. 21, 2019 [Dec. 12, 2022].

[23] S.-R. Tsai and M. R. Hamblin, "Biological Effects and Medical Applications of Infrared Radiation," *Journal of Photochemistry and Photobiology B: Biology,* vol. 170, pp. 197-207, May 2017.

[24] A. Barth, "Infrared Spectroscopy of Proteins," *Biochimica et Biophysica Acta (BBA) - Bioenergetics,* vol. 1767, no. 9, pp. 1073-101, September 2007.

[25] M. Jordi Taltavull, "The Uncertain Limits Between Classical and Quantum Physics: Optical Dispersion and Bohr's Atomic Model," *Annalen der Physik,* vol. 530, no. 8, p. 1800104, August 2018.

[26] Harpreet_Physics, "What is Stimulated Emission?" https://www.goseeko.com/blog/what-is-stimulated-emission, Aug. 3, 2021 [Dec. 16, 2022].

[27] M. Koç and E. Karabudak, "History of Spectroscopy and Modern Micromachined Disposable Si ATR-IR Spectroscopy," *Applied Spectroscopy Reviews,* vol. 53, no. 5, pp. 420-38, May 2018.

[28] X. Liu, "Infrared (IR) Spectroscopy Theory." https://kpu.pressbooks.pub/organicchemistry/chapter/6-2-infrared-ir-spectroscopy, Dec. 19, 2021 [Dec. 18, 2022].

[29] D. C. Giancoli, *Physics for Scientists & Engineers with Modern Physics*, 4th ed. Harlow, Essex: Pearson, 2014, 667-8.

[30] BYJU'S, "Work Done To Rotate A Dipole In External Electric Uniform Field." https://byjus.com/physics/work-done-to-rotate-a-dipole-in-external-electric-uniform-field, Aug. 18, 2022 [Dec. 20, 2022].

[31] C. Berthomieu and R. Hienerwadel, "Fourier Transform Infrared (FTIR) Spectroscopy," *Photosynthesis Research,* vol. 101, no. 2, pp. 157-70, September 2009.

[32] J. M. Parnis and K. B. Oldham, "Beyond the Beer–Lambert Law: The Dependence of Absorbance on Time in Photochemistry," *Journal of Photochemistry and Photobiology A: Chemistry,* vol. 267, pp. 6-10, September 2013.

[33] "Definition of Fourier Transform Infrared Spectrometer (FTIR)." https://www.chemicool.com/definition/fourier_transform_infrared_spectrometer_ftir.html, [Dec. 21, 2022].

[34] N. B. Colthup, L. H. Daly, and S. E. Wiberley, *Introduction to Infrared and Raman Spectroscopy*, 3rd ed. Boston: Academic Press, 1990, 315, 318, 320-2, 325, 329, 331, 334, 345, 363, 365-6, 373-6, 387-8, 391-2, 394, 441.

[35] J. Grdadolnik, "Conformation of Bovine Serum Albumin as a Function of Hydration Monitored by Infrared Spectroscopy," *The Internet journal of vibrational spectroscopy,* vol. 6, no. 1, 6, pp. 1-13, 2002.

[36] M. T. Larsen, M. Kuhlmann, M. L. Hvam, and K. A. Howard, "Albumin-based Drug Delivery: Harnessing Nature to Cure Disease," (in eng), *Molecular and Cellular Therapies,* vol. 4, p. 3, February 2016.